Trojan Nuclear Plant
Docket 50-344
License NPF-1

Document Control Desk
March 14, 1988
Attachment B

[redacted]

FOR UNRESTRICTED DISTRIBUTION
DATE _____ WEC

[redacted]

Westinghouse Energy Systems

8803210005 880314
PDR ADOCK 05000344
P DCD

WCAP-11700

TECHNICAL JUSTIFICATION FOR ELIMINATING LARGE PRIMARY LOOP PIPE RUPTURE AS THE STRUCTURAL DESIGN BASIS FOR THE TROJAN PLANT

FEBRUARY 1988

S. A. Swamy
E. R. Johnson F. J. Witt
C. C. Kim C. B. Bond
V. M. Bhambri Y. S. Lee

Verified by: G. C. Schmertz

Approved by: S. S. Palusamy, Manager
Structural Materials Engineering

Work Performed Under Shop Order PPLJ950

WESTINGHOUSE ELECTRIC CORPORATION
Generation Technology Systems Division
P.O. Box 2728
Pittsburgh, Pennsylvania 15230-2728

TABLE OF CONTENTS

TABLE OF CONTENTS (Cont'd.)

LIST OF TABLES

LIST OF TABLES (Cont'd.)

LIST OF FIGURES

LIST OF FIGURES (Cont'd.)

PREFACE

Portland General Electric Company submitted a leak-before-break analysis for the elimination of primary loop pipe ruptures for the Trojan Nuclear plant (Impell Report No. 01-0300-1395, Rev. 1).

After completing their review, the NRC transmitted to Portland General Electric Company a request for additional information. Portland General Electric Company contracted with Westinghouse Electric Corporation to respond to the NRC request including the performance of analyses. This report presents a detailed leak-before-break evaluation including the response to the NRC request. The NRC request is reproduced here:

REQUEST FOR ADDITIONAL INFORMATION ON ELIMINATION OF POSTULATED PRIMARY LOOP PIPE RUPTURES AS A DESIGN BASIS

By letter dated October 31, 1986, Portland General Electric Company (the licensee) submitted the technical basis for the elimination of primary loop pipe ruptures using "leak-before-break" (LBB) methodology for the Trojan Nuclear Plant in Impell Report No. 01-0300-1395, Rev. 1, dated October 1986. The staff has reviewed the licensee's submittal for compliance with the revised General Design Criterion 4 (GDC-4) of appendix A, 10 CFR 50. The evaluation criteria are discussed in detail in NUREG-1061, Volume 3. The staff requires the following additional information from the licensee before our review can continue.

(1) The LBB criteria in NUREG-1061, Volume 3 contain margins on leakage rate, crack size, and applied loads to account for uncertainties inherent in the analyses. The LBB margins are discussed in detail in NUREG-1061, Volume 3. The margins on crack size and applied loads were not addressed by the licensee in the submitted report. The licensee should discuss compliance with the margin of 2 on the crack size and the margin of "the square root of 2" on the applied loads. The licensee should demonstrate the stability of a through-wall crack twice the size of the leakage-size crack under

combined normal and safe shutdown earthquake (SSE) loads. Also, the licensee should demonstrate the stability of the leakage-size crack if the loads are increased to the square root of 2 times the combination of normal and SSE loads.

(2) In Section 2.5.1 of the submitted report, the Licensee discussed the thermal aging effects of cast stainless steel on the material fracture toughness. However, the specific extent of thermal aging depends on the chemistry and the ferrite content of the cast material. The licensee should demonstrate that the data shown in figure 5 of the submitted report provide a lower-bound estimate of the toughness properties for the specific Trojan material. Alternatively, the licensee should determine the thermally-aged fracture toughness for each cast stainless steel piping component material in the primary loop of Trojan based on its specific chemistry and the ferrite content.

(3) The LBB analysis should be performed for the functional piping system from anchor point to anchor point. In figure 1 of the submitted report, it is indicated that LBB analyses were performed at break locations. In Section 2.4.1 of the submitted report, the licensee indicated that several intermediate locations were also considered. The LBB methodology should be separated from the methodology in Standard Review Plan 3.6.2 which discusses break locations. In the application of LBB, the piping system from anchor to anchor, including all intermediate locations, should be considered. The limiting location for LBB analyses is the location with the highest stresses coincident with the poorest material properties for base materials, weldments, and safe ends. The effects of thermal aging as discussed in item 2 above must be considered.

(4) Linear elastic fracture mechanics (LEFM) was used for the fracture stability analysis. However, from the calculated fracture mechanics parameter "J-integral", it appears that the associated Irwin plane-stress plastic zone sizes are not small, compared with the

half-crack length. The licensee should use elastic-plastic fracture mechanics (EPFM) instead of LEFM procedures. Although the licensee attempted to compare the plastic zone with the uncracked circumference in table 6 of the submitted report, the proper comparison should be with the crack length because the crack length is less than the uncracked circumference. Furthermore, the licensee should benchmark the EPFM procedure against experimental pipe test data.

(5) In Section 2.4.1 of the submitted report, it is indicated that SSE loads were obtained by multiplying the maximum operating basis earthquake (OBE) loads by a factor of 1.67. Describe the validity of obtaining SSE loads from OBE loads.

(6) In Section 2.5.2 of the submitted report, it is indicated that four typical weld procedures were reviewed to determine the welding process of the primary loop. From this review, the licensee determined that the welding processes were shielded metal arc welding (SMAW) and gas-tungsten arc welding (GTAW). The licensee should review all the welding procedures for the primary loop to determine if submerged arc welds (SAW) were used. Also, indicate if solution annealing was performed. Furthermore, the staff disagrees with the licensee's assertion in Section 2.5.3 of the submitted report that the fracture toughness of GTAW would bound that of SMAW.

(7) In Section 2.4.2 of the submitted report, it is indicated that ASME Code minimum material properties were used. Because various materials were used in the fabrication of the primary loop, describe the Code minimum of which material was used for the calculation and justify this selection. Also, provide the elastic modulus, yield strength, ultimate strength, and stress-strain curve at the limiting location and at the operating temperature. The licensee would have to select these material properties in order to perform a EPFM evaluation as discussed in item 4 above.

(8) In Section 2.4.2 of the submitted report, the licensee indicated that a fully-plastic displacement-controlled tearing modulus (J-T) analysis was performed. Describe whether the J-T result shown in figure 8 of the submitted report was calculated for a 7-inch crack in the hot leg vessel outlet nozzle. If the calculation was based on a 25-inch crack as discussed in Section 2.4.2 of the submitted report, it is not conservative to use the J-integral value for a 7-inch crack on the J-T curve for a 25-inch crack. Also, the licensee should use elastic-plastic load-controlled J-T analysis because a fully-plastic displacement-controlled J-T analysis may not be conservative. Furthermore, if crack growth is predicted before instability, crack growth should be considered in the J-T analysis.

(9) In appendix A of the submitted report, the licensee indicated that the leakage prediction computer code has been benchmarked against test data. The licensee should submit the benchmarking results for staff review.

(10) In table 1 of the submitted report, the licensee listed the diameters and wall thicknesses of the hot leg, crossover leg, and the cold leg. Describe whether the nominal dimensions or minimum dimensions were tabulated. If nominal dimensions were used, the licensee should review the as-built configuration of the primary loop weldments to determine whether the actual thickness is less than the nominal thickness. Due to weld fit-up, the actual thickness may be less than the nominal pipe thickness.

(11) In appendix C of the submitted report, a fatigue crack growth analysis was discussed. Describe the design transients considered in the analysis. Also, show the crack growth material data used for the analysis.

(12) Net section plastic analysis was discussed in Section 2.6 of the submitted report. However, net section analysis does not account for material toughness limitations. In particular, low toughness thermally-aged cast stainless steel is involved in the present LBB evaluation. The licensee should use a fracture stability analysis which accounts for material toughness.

SUMMARY RESPONSE

This report includes detailed response to the above requests. A summary of responses is provided below by addressing each request individually.

Request 1

The response to this request is given in Section 6.3. The margins on crack size and loads are discussed in detail in Section 6.3 and Section 8.0.

Request 2

The thermally-aged fracture toughness (end of life) for each cast stainless steel piping component material in the primary loop of the Trojan plant was established based on its chemistry and ferrite content. Details are provided in Section 4.3 and Appendix B.

Request 3

The entire primary loop (from anchor to anchor) was considered in the evaluation. Five critical locations were identified based on detailed review of loads, material chemistry and material properties for the entire system (Sections 3 and 4). Effects of thermal aging have been addressed in detail. (Sections 4 and Appendix B).

Request 4

Elastic plastic fracture mechanics (EPFM) was used for determining J_{app} and T_{app} in the stability analyses of Section 6.0. Thus, the analyses of Section 6.0 comply with this request.

Request 5

The response to this request is provided in Section 3.2.

Request 6

The response to this request is provided in Section 4.0.

Request 7

Representative minimum and average properties were established based on Trojan plant specific material certification records. Lower-bound (minimum) properties were used for crack stability analyses and average properties were used for leak rate predictions. All the information requested is provided in Section 4.0.

Request 8

Elastic-plastic load controlled J-T analyses were performed. Detailed discussion is provided in Section 6.0.

Request 9

The Westinghouse computer code for calculating leak rates has been benchmarked and placed under Configuration Control. Results of benchmark calculations have been reviewed and accepted by the NRC in connection with other LBB applications.

Request 10

The minimum wall-thicknesses at weld undercuts were used in the calculations presented in this report (Section 3.0).

Request 11

Typical design transients are listed in Table 7-1 of this report. The crack growth rate data used for the fatigue crack growth analysis is provided in Section 7.0.

Request 12

Limit load analyses do not produce limiting flaw sizes and such results have no impact on the governing stability and margin evaluations presented in this report. Fracture stability analyses which account for material toughness are presented in this report. Thus, the analyses presented comply with this request.

SECTION 1.0
INTRODUCTION

1.1 Purpose

This report applies to the Trojan Nuclear Power Plant Reactor Coolant System (RCS) primary loop piping. It is intended to demonstrate that for the specific parameters of the Trojan plant, RCS primary loop pipe breaks need not be considered in the structural design basis. The approach taken has been accepted by the Nuclear Regulatory Commission (NRC) (reference 1-1).

1.2 Scope

The existing structural design basis for the RCS primary loop requires that dynamic effects of pipe breaks be evaluated. In addition, protective measures for the dynamic effects associated with RCS primary loop pipe breaks have been incorporated in the Trojan plant design. However, Westinghouse has demonstrated on a generic basis that RCS primary loop pipe breaks are highly unlikely and should not be included in the structural design basis of Westinghouse plants (see reference 1-2). In order to demonstrate this applicability of the generic evaluations to the Trojan plant, Westinghouse has performed a fracture mechanics evaluation, a determination of leak rates from a through-wall crack, a fatigue crack growth evaluation, and an assessment of margins.

1.3 Objectives

In order to validate the elimination of RCS primary loop pipe breaks for the Trojan plant, the following objectives must be achieved:

a. Demonstrate that margin exists between the "critical" crack size and a postulated crack which yields a detectable leak rate.

b. Demonstrate that there is sufficient margin between the leakage through a postulated crack and the leak detection capability of the Trojan plant.

c. Demonstrate margin on applied load.

d. Demonstrate that fatigue crack growth is negligible.

1.4 Background Information

Westinghouse has performed considerable testing and analysis to demonstrate that RCS primary loop pipe breaks can be eliminated from the structural design basis of ail Westinghouse plants. The concept of eliminating pipe breaks in the RCS primary loop was first presented to the NRC in 1978 in WCAP-9283 (reference 1-3). That Topical Report employed a deterministic fracture mechanics evaluation and a probabilistic analysis to support the elimination of RCS primary loop pipe breaks. That approach was then used as a means of addressing Generic Issue A-2 and Asymmetric LOCA Loads.

Westinghouse performed additional testing and analysis to justify the elimination of RCS primary loop pipe breaks. This material was provided to the NRC along with Letter Report NS-EPR-2519 (reference 1-4).

The NRC funded research through Lawrence Livermore National Laboratory (LLNL) to address this same issue using a probabilistic approach. As part of the LLNL research effort, Westinghouse performed extensive evaluations of specific plant loads, material properties, transients, and system geometries to demonstrate that the analysis and testing previously performed by Westinghouse and the research performed by LLNL applied to all Westinghouse plants (references 1-5 and 1-6). The results from the LLNL study were released at a March 28, 1983 ACRS Subcommittee meeting. These studies which are applicable to all Westinghouse plants east of the Rocky Mountains determined the mean probability of a direct LOCA (RCS primary loop pipe break) to be 4.4×10^{-12} per reactor year and the mean probability of an indirect LOCA to be 10^{-7} per reactor year. Thus, the results previously obtained by Westinghouse (reference 1-3) were confirmed by an independent NRC research study.

To determine if the probability of double ended guillotine breaks is small enough for the plants located on the west coast also, the NRC contracted with the LLNL to conduct a probabilistic assessment of the primary coolant loop piping of the west coast plants. The study performed by LLNL included a plant specific evaluation of the Trojan plant (reference 1-7). That evaluation determined the mean probability of a direct LOCA (RCS primary loop pipe break) to be 2.2×10^{-13} per reactor year. It should be noted that the plant specific probability of a direct LOCA for the Trojan plant, 2.2×10^{-13} is even lower than the mean probability of all the Westinghouse plants east of the Rocky Mountains.

Based on the studies by Westinghouse, LLNL, the ACRS, and the AIF, the NRC completed a safety review of the Westinghouse reports submitted to address asymmetric blowdown loads that result from a number of discrete break locations on the PWR primary systems. The NRC Staff evaluation (reference 1-1) concludes that an acceptable technical basis has been provided so that asymmetric blowdown loads need not be considered for those plants that can demonstrate the applicability of the modeling and conclusions contained in the Westinghouse response or can provide an equivalent fracture mechanics demonstration of the primary coolant loop integrity. In a more formal recognition of LBB methodology applicability for PWRs, the NRC appropriately modified 10CFR50, General Design Criterion 4, "Requirements for Protection Against Dynamic Effects for Postulated Pipe Rupture" (51FR 12502).

This report provides a fracture mechanics demonstration of primary loop integrity for the Trojan plant consistent with the NRC position for exemption from consideration of dynamic effects.

Several computer codes are used in the evaluations. The main-frame computer programs are under Configuration Control which has requirements conforming to Standard Review Plan 3.9.1. The fracture mechanics calculations are independently verified (benchmarked).

1.5 References

1-1 USNRC Generic letter 84-04, Subject: "Safety Evaluation of Westinghouse Topical Reports Dealing with Elimination of Postulated Pipe Breaks in PWR Primary Main Loops," February 1, 1984.

1-2 Letter from Westinghouse (E. P. Rahe) to NRC (R. H. Vollmer), NS-EPR-2768, dated May 11, 1983.

1-3 WCAP-9283, "The Integrity of Primary Piping Systems of Westinghouse Nuclear Power Plants During Postulated Seismic Events," March, 1978.

1-4 Letter Report NS-EPR-2519, Westinghouse (E. P. Rahe) to NRC (D. G. Eisenhut), Westinghouse Proprietary Class 2, November 10, 1981.

1-5 Letter from Westinghouse (E. P. Rahe) to NRC (W. V. Johnston) dated April 25, 1983.

1-6 Letter from Westinghouse (E. P. Rahe) to NRC (W. V. Johnston) dated July 25, 1983.

1-7 NUREG/CR-3660, Vol. 4, UCID-19988, Vol. 4, "Probability of Pipe Failure in the Reactor Coolant Loops of Westinghouse PWR Plants Volume 4: Pipe Failure Induced by Crack Growth in West Coast Plants," July 1985.

SECTION 2.0
OPERATION AND STABILITY OF THE REACTOR COOLANT SYSTEM

2.1 Stress Corrosion Cracking

The Westinghouse reactor coolant system primary loops, have an operating history that demonstrates the inherent operating stability characteristics of the design. This includes a low susceptibility to cracking failure from the effects of corrosion (e.g., intergranular stress corrosion cracking). This operating history totals over 400 reactor-years, including five plants each having over 15 years of operation and 15 other plants each with over 10 years of operation.

In 1978, the United States Nuclear Regulatory Commission (USNRC) formed the second Pipe Crack Study Group. (The first Pipe Crack Study Group established in 1975 addressed cracking in boiling water reactors only.) One of the objectives of the second Pipe Crack Study Group (PCSG) was to include a review of the potential for stress corrosion cracking in Pressurized Water Reactors (PWR's). The results of the study performed by the PCSG were presented in NUREG-0531 (reference 2-1) entitled "Investigation and Evaluation of Stress Corrosion Cracking in Piping of Light Water Reactor Plants." In that report the PCSG stated:

> "The PCSG has determined that the potential for stress-corrosion cracking in PWR primary system piping is extremely low because the ingredients that produce IGSCC are not all present. The use of hydrazine additives and a hydrogen overpressure limit the oxygen in the coolant to very low levels. Other impurities that might cause stress-corrosion cracking, such as halides or caustic, are also rigidly controlled. Only for brief periods during reactor shutdown when the coolant is exposed to the air and during the subsequent startup are conditions even marginally capable of producing stress-corrosion cracking in the primary systems of PWRs. Operating experience in PWRs supports this determination. To date, no stress-corrosion cracking has been reported in the primary piping or safe ends of any PWR."

During 1979, several instances of cracking in PWR feedwater piping led to the establishment of the third PCSG. The investigations of the PCSG reported in NUREG-0691 (reference 2-2) further confirmed that no occurrences of IGSCC have been reported for PWR primary coolant systems.

As stated above, for the Westinghouse plants there is no history of cracking failure in the reactor coolant system loop. The discussion below further qualifies the PCSG's findings.

For stress corrosion cracking (SCC) to occur in piping, the following three conditions must exist simultaneously: high tensile stresses, susceptible material, and a corrosive environment. Since some residual stresses and some degree of material susceptibility exist in any stainless steel piping, the potential for stress corrosion is minimized by properly selecting a material immune to SCC as well as preventing the occurrence of a corrosive environment. The material specifications consider compatibility with the system's operating environment (both internal and external) as well as other material in the system, applicable ASME Code rules, fracture toughness, welding, fabrication, and processing.

The elements of a water environment known to increase the susceptibility of austenitic stainless steel to stress corrosion are: oxygen, fluorides, chlorides, hydroxides, hydrogen peroxide, and reduced forms of sulfur (e.g., sulfides, sulfites, and thionates). Strict pipe cleaning standards prior to operation and careful control of water chemistry during plant operation are used to prevent the occurrence of a corrosive environment. Prior to being put into service, the piping is cleaned internally and externally. During flushes and preoperational testing, water chemistry is controlled in accordance with written specifications. Requirements on chlorides, fluorides, conductivity, and pH are included in the acceptance criteria for the piping.

During plant operation, the reactor coolant water chemistry is monitored and maintained within very specific limits. Contaminant concentrations are kept below the thresholds known to be conducive to stress corrosion cracking with the major water chemistry control standards being included in the plant operating procedures as a condition for plant operation. For example, during

normal power operation, oxygen concentration in the RCS is expected to be in the ppb range by controlling charging flow chemistry and maintaining hydrogen in the reactor coolant at specified concentrations. Halogen concentrations are also stringently controlled by maintaining concentrations of chlorides and fluorides within the specified limits. Thus during plant operation, the likelihood of stress corrosion cracking is minimized.

2.2 Water Hammer

Overall, there is a low potential for water hammer in the RCS since it is designed and operated to preclude the voiding condition in normally filled lines. The reactor coolant system, including piping and primary components, is designed for normal, upset, emergency, and faulted condition transients. The design requirements are conservative relative to both the number of transients and their severity. Relief valve actuation and the associated hydraulic transients following valve opening are considered in the system design. Other valve and pump actuations are relatively slow transients with no significant effect on the system dynamic loads. To ensure dynamic system stability, reactor coolant parameters are stringently controlled. Temperature during normal operation is maintained within a narrow range by control rod position; pressure is controlled by pressurizer heaters and pressurizer spray also within a narrow range for steady-state conditions. The flow characteristics of the system remain constant during a fuel cycle because the only governing parameters, namely system resistance and the reactor coolant pump characteristics, are controlled in the design process. Additionally, Westinghouse has instrumented typical reactor coolant systems to verify the flow and vibration characteristics of the system. Preoperational testing and operating experience have verified the Westinghouse approach. The operating transients of the RCS primary piping are such that no significant water hammer can occur.

2.3 Low Cycle and High Cycle Fatigue

Low cycle fatigue considerations are accounted for in the design of the piping system through the fatigue usage factor evaluation to show compliance with the rules of Section III of the ASME Code. A further evaluation of the low cycle fatigue loadings was carried out as part of this study in the form of a fatigue crack growth analysis, as discussed in Section 7.

High cycle fatigue loads in the system would result primarily from pump vibrations. These are minimized by restrictions placed on shaft vibrations during hot functional testing and operation. During operation, an alarm signals the exceedance of the vibration limits. Field measurements have been made on a number of plants during hot functional testing, including plants similar to Trojan. Stresses in the elbow below the reactor coolant pump resulting from system vibration have been found to be very small, between 2 and 3 ksi at the highest. These stresses are well below the fatigue endurance limit for the material and would also result in an applied stress intensity factor below the threshold for fatigue crack growth.

2.4 References

2-1 Investigation and Evaluation of Stress-Corrosion Cracking in Piping of Light Water Reactor Plants, NUREG-0531, U.S. Nuclear Regulatory Commission, February 1979.

2-2 Investigation and Evaluation of Cracking Incidents in Piping in Pressurized Water Reactors, NUREG-0691, U.S. Nuclear Regulatory Commission, September 1980.

SECTION 3.0
PIPE GEOMETRY AND LOADING

The general analytical approach is discussed first. A segment of the primary coolant hot leg pipe shown below to be limiting in terms of stresses is sketched in figure 3-1. This segment is postulated to contain a circumferential through-wall flaw. The inside diameter and minimum wall thickness of the pipe at the weld undercut are 29.2 and 2.33 inches, respectively. The pipe is subjected to a normal operating pressure of 2235 psig. Figure 3-2 identifies the loop weld locations. The material properties and the loads at these locations resulting from deadweight, thermal expansion, and Safe Shutdown Earthquake are evaluated. The junction of the hot leg and the reactor vessel outlet nozzle is the worst location for crack stability analysis based on the highest stress due to combined pressure, dead weight, thermal expansion, and SSE (Safe Shutdown Earthquake) loadings. At this location, the axial load (F_x) and the bending moment (M_b) are 1918 kips (including axial force due to pressure) and 31,795 in-kips, respectively. This location is referred to as the load critical location. However, as seen later, significant degradation of end-of-service life fracture toughnesses due to thermal aging occurs in some of the pipe heats and fittings. The highest stresses and lowest toughness locations for which pipes fittings suffer such degradation are referred to as toughness critical locations. The associated heats of material or welds with low toughness are called the toughness critical materials. The toughness critical locations are 3, 7, 9 and 11 (see figure 3-2).

The stresses due to axial loads and bending moments are calculated by the following equation:

$$\sigma = \frac{F}{A} + \frac{M}{Z} \qquad (3.1)$$

where,

σ = stress
F = axial load
M = bending moment
A = metal cross-sectional area
Z = section modulus

The bending moments for the desired loading combinations are calculated by the following equation:

$$M = \sqrt{M_Y^2 + M_Z^2} \qquad (3.2)$$

where,

M = bending moment for required loading
M_Y = Y component of bending moment
M_Z = Z component of bending moment

The axial load and bending moments for leak rate predictions and crack stability analysis are computed by the methods to be explained in Sections 3.1, 3.2 and 3.3.

3.1 Loads for Leak Rate Evaluation

The normal operating loads for leak rate predictions are calculated by the following equations:

$$F = F_{DW} + F_{TH} + F_P \qquad (3.3)$$

$$M_Y = (M_Y)_{DW} + (M_Y)_{TH} + (M_Y)_P \qquad (3.4)$$

$$M_Z = (M_Z)_{DW} + (M_Z)_{TH} + (M_Z)_P \qquad (3.5)$$

The subscripts of the above equations represent the following loading cases:

DW = deadweight
TH = normal thermal expansion
P = load due to internal pressure

The loads based on this method of combination are provided in table 3-1 for all the critical locations (load critical as well as toughness critical.)

3.2 Loads for Crack Stability Analysis

The faulted loads for the crack stability analysis are calculated by the following equations:

$$F = |F_{DW} + F_{TH} + F_P| + |F_{SSE}| \quad (3.6)$$

$$M_Y = |(M_Y)_{DW} + (M_Y)_{TH} + (M_Y)_P| + |(M_Y)_{SSE}| \quad (3.7)$$

$$M_Z = |(M_Z)_{DW} + (M_Z)_{TH} + (M_Z)_P| + |(M_Z)_{SSE}| \quad (3.8)$$

Where the subscript SSE represents SSE loading including seismic anchor motion. For the above load combination, the SSE (inertia) and SSE (anchor motion) are combined by the square-root-sum-of-the-squares method. The loads based on this method of combination are provided in table 3-2 for all the critical locations (load critical as well as toughness critical).

The seismic response spectra for the Trojan plant were generated for the OBE event by Bechtel Corporation and provided to Westinghouse for seismic analysis of the primary coolant loop. The response spectra for the SSE (DBE) event have been calculated on a conservative basis by multiplying the OBE spectra by the ratio of DBE to OBE peak ground acceleration. The calculated ratio is 0.25 g's divided by 0.15 g's or 1.67. Lower magnitude SSE spectra, based on higher structural damping for SSE than for OBE, were not generated or used in the loop seismic analysis.

The seismic analysis of the primary coolant loop consists of two portions: inertia response of the primary coolant loop (steam generator, reactor coolant pump, hot leg, crossover leg and cold leg piping); and static anchor motion response for the reactor pressure vessel displacement. The building static anchor motions for SSE are negligibly small (only 0.010 inches of relative horizontal displacement). The damping values used in the SSE analysis are 0.5% for the inertia response of the primary coolant loop and 2.0% for the inertia response of the reactor pressure vessel. These correspond to FSAR values for vital piping and welded structures, respectively.

3.3 Alternate Load Combination for Crack Stability Analysis Based on Absolute Summation

In accordance with draft standard review plan 3.6.3 an alternate combination of loading components can be applied which results in higher magnitude of combined loads. If crack stability is demonstrated using these loads, the LBB margin on loads can be reduced from $\sqrt{2}$ to 1.0. The absolute summation of loads results in the following equations:

$$F = |F_{DW}| + |F_{TH}| + |F_P| + |F_{SSEINERTIA}| + |F_{SSEAM}| \quad (3.9)$$

$$M_Y = |(M_Y)_{DW}| + |(M_Y)_{TH}| + |(M_Y)_P| + |(M_Y)_{SSEINERTIA}| + |(M_Y)_{SSEAM}| \quad (3.10)$$

$$M_Z = |(M_Z)_{DW}| + |(M_Z)_{TH}| + |(M_Z)_P| + |(M_Z)_{SSEINERTIA}| + |(M_Z)_{SSEAM}| \quad (3.11)$$

Based on this method of combination, the loads at the highest stressed location (i.e. location 1 - reactor vessel outlet nozzle junction) are:

F_x = 2235 kips, M_b = 34,716 in-kips.

These loads are used in the fracture mechanics evaluations (section 6.0) to demonstrate margin on loads at location 1.

TABLE 3-1

NORMAL CONDITION (DEAD WEIGHT AND PRESSURE AND THERMAL) LOADS FOR TROJAN

Weld Location	Axial Load Fx (kips)[a]	Bending Moment Mb (in-kips)
1[b]	1438	24,754
3	1572	16,689
7	1695	4,372
9	1785	12,346
11	1363	5,945

---

a) Includes internal pressure

b) Load critical location. Remaining locations are toughness critical locations.

TABLE 3-2

TROJAN PRIMARY LOOP DATA INCLUDING FAULTED LOADING CONDITIONS

Weld Locations	Inside Radius (in)	Wall Thickness (in)	Yield Stress σ_y (ksi)	Ultimate Stress σ_u (ksi)	[Flow Stress (ksi)]a,c,e	Faulted Loads[a] Axial Load (Kips) F_x	Faulted Loads[a] Bending Moment (in-Kips) M_b	Direct Stress (ksi) $\sigma_a = \frac{F_x}{A} + \frac{M_b}{Z}$
1[b]	14.6	2.33	20.4	60.0	40.2	1918	31795	26.98
3[c]	15.6	2.48	23.8	52.9	38.4	2053	26432	20.59
7[c]	15.6	2.48	24.7	52.9	38.8	1798	8901	11.15
9[c]	15.6	2.48	24.7	52.9	38.8	1901	15634	14.80
11[c]	13.85	2.21	21.1	60.0	40.6	2146	11832	18.47

[a] Includes internal pressure

[b] Load critical location for the entire system

[c] Toughness critical location

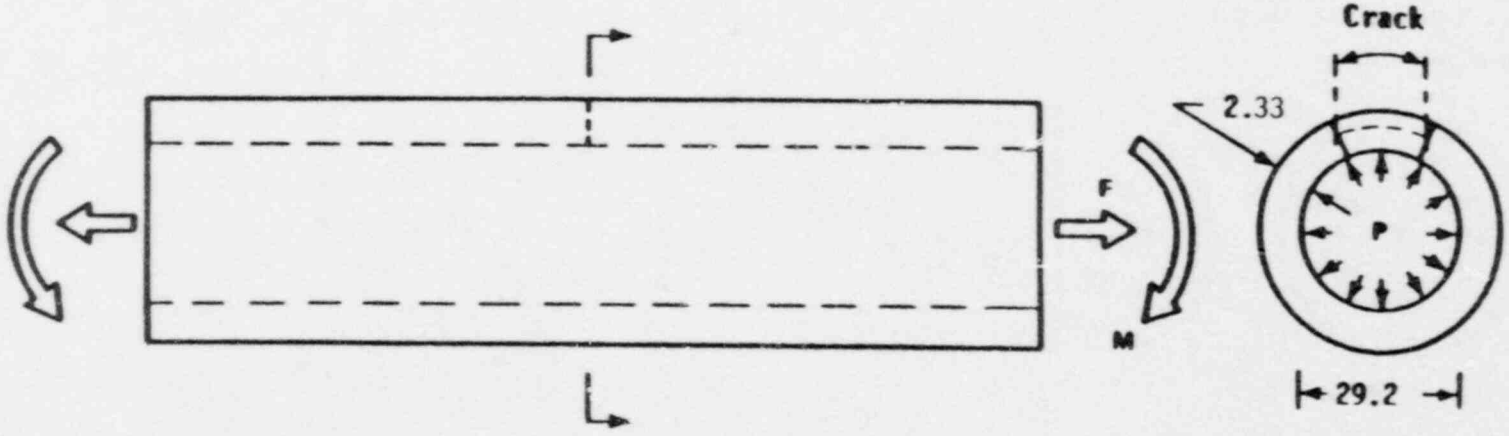

P = 2,235 psig
F = 1918 kips
M = 31,795 in-kips

Figure 3-1 Reactor Coolant Pipe

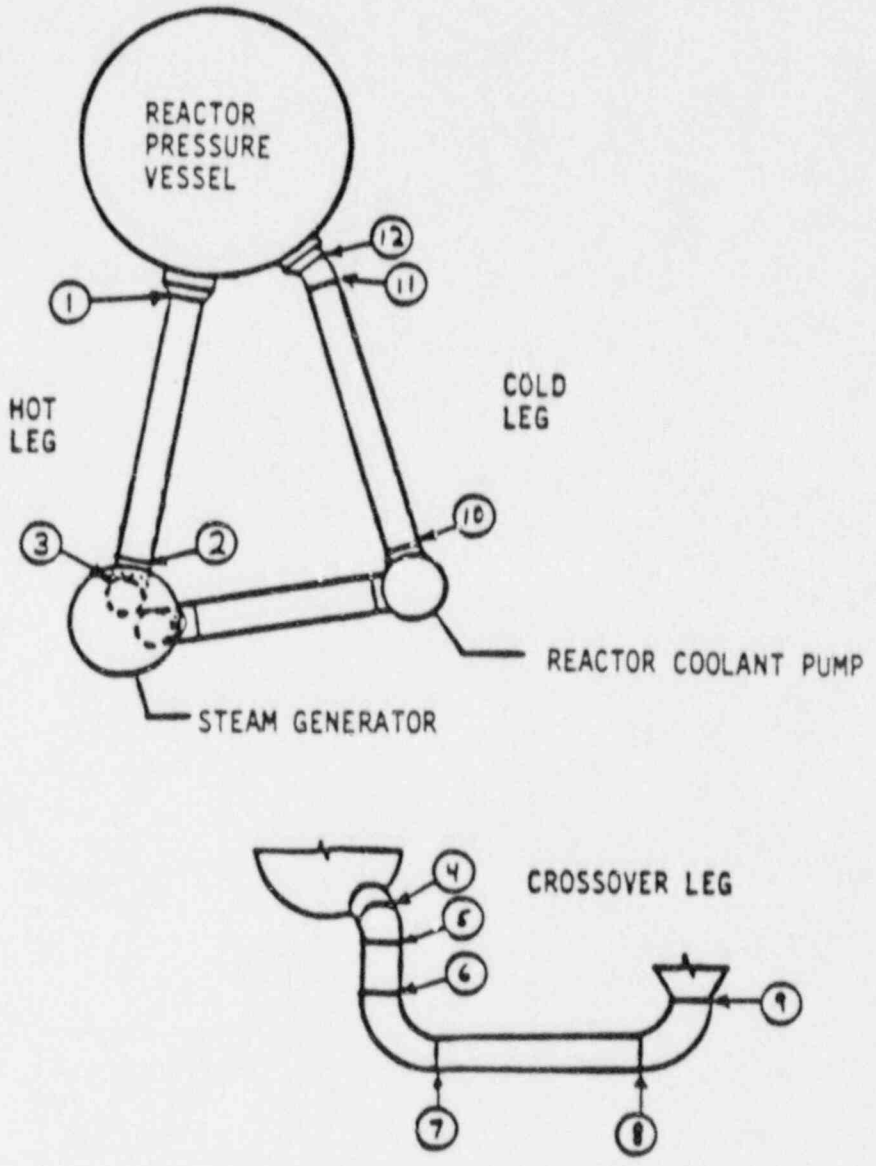

Figure 3-2 Schematic Diagram of Trojan RCL Showing Weld Identifications

SECTION 4.0
MATERIAL CHARACTERIZATION

4.1 Primary Loop Pipe and Fittings Materials

The primary loop piping for the Trojan plant is SA351 CF8A. The piping is centrifugally cast while the fittings are statically cast. The elbow fittings are made of SA351 CF8M material. The field welds feature a gas tungsten arc weld (GTAW or TIG) root pass followed by shielded metal arc welding (SMAW) to completion. The shop welds are either SMAW or submerged arc (SAW) with a GTAW root pass. Weld repairs on shop welds would be either SMAW or GTAW. The welds have TP 308 stainless steel chemistry. No solution annealing was performed.

4.2 Tensile Properties

Plant specific material certifications were used to establish the tensile properties for the leak-before-break analyses. Table 4-1 shows the tensile properties of the SA351 CF8A material at 70°F and 650°F, as well as the properties of SA351 CF8M at 70°F, as taken from the material certifications. The properties of SA351 CF8A at 650°F from table 4-1 were used to obtain the representative minimum and average tensile properties of these materials at 650°F. Properties at operating temperature were not available for the CF8M material in the Trojan plant. [

]^{a,c,e} In table 4-4, the representative minimum and average properties of materials in the Trojan plant primary loop are summarized. In that table the ASME Code minimum properties are also included for a comparison.

Table 4-5 shows the temperature and pressure conditions in the primary loop. At location 1 of figure 3-2, for example, the normal operating temperature is 617°F. [

]^{a,c,e} In brief, the following material properties were the ones used in the leak-before-break analyses set forth in this report.

Minimum SA351 CF8A Properties for Flaw Stability Analysis for Location 1 (617°F)

[ ]^{a,c,e}

Average SA351 CF8A Properties for Leak Rate Calculations for Location 1 (617°F)

[ ]^{a,c,e}

Minimum SA351 CF8M Properties for Flaw Stability Analysis for Location 3 (617°F)

[ ]^{a,c,e}

Average SA351 CF8M Properties for Leak Rate Calculations for Location 3 (617°F)

[ ]a,c,e

Minimum SA351 CF8M Properties for Flaw Stability Analysis for Locations 7 and 9 (552°F)

[ ]a,c,e

Average SA351 CF8M Properties for Leak Rate Calculations for Locations 7 and 9 (552°F)

[ ]a,c,e

Minimum SA351 CF8A Properties for Flaw Stability Analysis for Location 11 (553°F)

[ ]a,c,e

Average SA351 CF8A Properties for Leak Rate Calculations for Location 11 (553°F)

[ ]a,c,e

4.3 Fracture Toughness Properties

The pre-service fracture toughness of cast materials in terms of J have been found to be very high at 600°F. Typical results for a cast material are given in figure 4-5 taken from reference 4-2. J_{Ic} is observed to be over 5000 in-lbs/in^2. However, cast stainless steels are subject to thermal aging during service. This thermal aging causes an elevation in the yield strength of the material and a degradation of the fracture toughness, the degree of degradation being proportional to the level of ferrite in the material.

To determine the effects of thermal aging on piping integrity, a detailed study was carried out in reference 4-3. In that report, fracture toughness results were presented for a material [

]^{a,c,e} The effects of the aging process on the end-of-service life fracture toughness are further discussed in appendix B.

End-of-service life toughness for the heats are established using the alternate toughness criteria methodology (appendix B). By that methodology a heat of material is said to be as good as [ ]^{a,c,e} if it can be demonstrated that its end-of-service fracture toughnesses equal or exceed those of [ ]^{a,c,e}. Of the forty-seven heats examined in appendix B, five are seen to be not as good as [ ]^{a,c,e}. The fracture toughness criteria to be used in the fracture mechanics evaluation, based on the alternate toughness methodology of appendix B, are given in table 4-5. These toughness values are the lowest of all heats occurring at the critical locations 1, 3, 7, 9 and 11, shown in figure 3-2.

Available data on aged stainless steel welds (references 4-3 and 4-4) indicate that J_{Ic} values for the worst case welds are of the same order as the aged material. However, the slope of the J-R curve is steeper, and higher J-values have been obtained from fracture tests (in excess of 3000 in-lb/in^2). The applied value of the J-integral for a flaw in the weld regions will be lower than that in the base metal because the yield stress for the weld materials is much higher at temperature[a]. Therefore, weld regions are less limiting than the cast material.

It is thus conservative to choose the end-of-service life toughness properties of [ ]^{a,c,e} as representative of those of the welds. Also, such pipes and fittings having an end-of-service life calculated room temperature charpy U-notch energy, (KCU), greater than that of [ ]^{a,c,e} are also conservatively assumed to have the properties of [ ]^{a,c,e}.

In the fracture mechanics analyses that follow, the fracture toughness properties given in table 4-6 will be used as the criteria against which the applied fracture toughness values will be compared.

---

[a] In the report all $J_{applied}$ values were conservatively determined by using base metal strength properties.

4.4 References

4-1 Nuclear Systems Materials Handbook, Part I - Structural Materials, Group 1 - High Alloy Steels, Section 2, ERDA Report TID 26666, November, 1975.

4-2 WCAP-9558 Rev. 2, "Mechanistic Fracture Evaluation of Reactor Coolant Pipe Containing a Postulated Circumferential Through-Wall Crack," Westinghouse Proprietary Class 2, June 1981.

4-3 WCAP-10456, "The Effects of Thermal Aging on the Structural Integrity of Cast Stainless Steel Piping for W NSSS," W Proprietary Class 2, November 1983.

4-4 Slama, G., Petrequin, P., Masson, S.H., and Mager, T.R., "Effect of Aging on Mechanical Properties of Austenitic Stainless Steel Casting and Welds", presented at SMiRT 7 Post Conference Seminar 6 - Assuring Structural Integrity of Steel Reactor Pressure Boundary Components, August 29/30, 1983, Monterey, CA.

4-5 Witt, F.J., Kim, C.C., "Toughness Criteria for Thermally Aged Cast Stainless Steel," WCAP-10931, Revision 1, Westinghouse Electric Corporation, July 1986, (Westinghouse Proprietary Class 2).

TABLE 4-1

MECHANICAL PROPERTIES OF THE PRIMARY LOOP MATERIALS OF THE TROJAN PLANT

PRODUCT FORM	HEAT NR	MATERIAL	0.2% OFFSET YIELD STRESS (PSI)		ULTIMATE STRENGTH (PSI)		% ELONGATION		% REDUCTION IN AREA	
			70°F	650°F	70°F	650°F	70°F	650°F	70°F	650°F
Straight Pipe	C1043	A351 CF8A	42,460	25,000	86,300	60,000	50.0	36.0	65.2	62.1
Straight Pipe	C1217	A351 CF8A	37,960	28,750	87,400	69,250	51.0	39.0	65.9	61.3
Straight Pipe	B2700-B	A351 CF8A	41,293	21,300	79,303	60,250	59.0	41.0	67.6	60.3
Straight Pipe	B2931	A351 CF8A	37,960	23,700	83,100	63,000	57.0	36.5	66.8	59.1
Straight Pipe	C1798-A	A351 CF8A	40,460	26,800	82,420	65,500	53.0	41.0	69.5	62.3
Straight Pipe	C1798-B	A351 CF8A	40,460	26,800	82,420	65,500	53.0	41.0	69.5	62.3
Straight Pipe	B2942	A351 CF8A	38,100	23,150	83,200	63,000	50.0	37.5	66.5	61.8
Straight Pipe	B2711	A351 CF8A	41,459	20,100	81,418	60,250	58.0	44.0	76.1	62.3
Straight Pipe	B2700-D	A351 CF8A	41,290	21,300	79,300	60,250	59.0	41.0	67.6	60.3
Straight Pipe	C1048	A351 CF8A	45,700	23,100	83,750	61,750	53.5	32.5	67.0	56.8
Straight Pipe	C2161-A	A351 CF8A	39,960	24,400	81,420	65,500	47.0	42.0	69.3	53.3
Straight Pipe	C2161-B	A351 CF8A	39,960	24,400	81,420	65,500	47.0	42.0	69.3	53.3
Straight Pipe	B2919	A351 CF8A	40,600	24,400	80,200	64,000	48.0	36.5	66.7	54.7
Straight Pipe	B2828	A351 CF8A	41,958	20,900	82,300	61,000	59.0	42.3	75.7	54.7
Straight Pipe	B2700-A	A351 CF8A	41,293	21,300	79,303	60,250	59.0	41.0	67.6	60.3
Straight Pipe	B2849	A351 CF8A	50,949	24,900	83,116	66,500	45.0	33.0	73.0	56.0
Straight Pipe	C1989-A	A351 CF8A	38,960	21,300	80,420	62,250	48.0	41.5	70.1	53.3
Straight Pipe	C1958-B	A351 CF8A	38,960	21,300	80,420	62,250	48.0	41.5	70.1	53.3
Straight Pipe	B2836	A351 CF8A	39,960	22,400	82,310	64,000	50.0	33.0	71.6	53.8
Straight Pipe	B2962	A351 CF8A	47,260	27,800	80,800	68,000	53.0	39.0	69.4	54.7
Straight Pipe	C1934-A	A351 CF8A	42,957	22,200	83,516	66,250	48.0	39.5	62.8	52.8
Straight Pipe	C1934-B	A351 CF8A	42,957	22,200	83,516	66,250	48.0	39.5	62.8	52.8
Straight Pipe	B2877	A351 CF8A	35,960	22,800	77,600	60,000	51.0	42.0	75.3	67.0
Straight Pipe	C1211	A351 CF8A	46,000	23,100	82,750	65,500	46.5	40.5	65.9	48.4
27-1/2" ID LR 22°ELL	41544-3	A351 CF8M	40,350		85,400		64.0		71.0	
22° ELL	41544-2	A351 CF8M	41,800		86,500		67.0		75.0	
22° ELL	41423-3	A351 CF8M	40,050		80,100		55.0		75.0	
27-1/2" ID LR 22°ELL	41423-2	A351 CF8M	37,100		79,900		65.0		72.0	
50° ELL	35222-1	A351 CF8M	48,320		86,820		49.0		70.0	
50° ELL	34749-1	A351 CF8M	34,900		71,100		61.0		73.0	

TABLE 4-1 (cont.)

MECHANICAL PROPERTIES OF THE PRIMARY LOOP MATERIALS OF THE TROJAN PLANT

PRODUCT FORM	HEAT NR	MATERIAL	0.2% OFFSET YIELD STRESS (PSI) 70°F	650°F	ULTIMATE STRENGTH (PSI) 70°F	650°F	% ELONGATION 70°F	650°F	% REDUCTION IN AREA 70°F	650°F
50° ELL	61969-1	A351 CF8M	42,000		88,250		58.0		73.0	
50° ELL	61969-2	A351 CF8M	42,000		88,250		58.0		73.0	
90° x 31" Elbow	65282-1	A351 CF8M	51,350		95,350		48.0		70.0	
31" ID LR 90°ELL Suc.	66035-1	A351 CF8M	41,850		82,200		49.0		69.0	
31" ID LR 90°Elbow	64849-1	A351 CF8M	50,250		85,000		54.0		73.0	
31" ID 90°Plenum Elbw	63317	A351 CF8M	40,850		81,150		52.0		72.0	
31" IDx90°Elbow	65118-1	A351 CF8M	44,900		88,300		48.0		71.0	
31" IDx90°Suct Elbw	67348-1	A351 CF8M	48,500		90,700		46.0		67.0	
31" ID LR 90°ELL	63190-1	A351 CF8M	42,000		84,000		44.0		71.0	
31" ID 90°Plenum Elbw	68774-1	A351 CF8M	42,100		81,950		48.0		67.0	
40°ELL	62648	A351 CF8M	40,850		87,000		65.0		69.0	
40°ELL	62554	A351 CF8M	43,050		89,100		56.0		71.0	

TABLE 4-2

MECHANICAL PROPERTIES OF SA351 CF8M MATERIAL
AT 650°F (FROM A TYPICAL PWR PLANT)

PRODUCT FORM	HEAT NR	TEST PIECE NR	MATERIAL	0.2% OFFSET YIELD STRESS (PSI)	ULTIMATE STRENGTH (PSI)	% ELONGATION	% REDUCTION IN AREA
90 DEG HALF ELBOW	4969	3/6	A351 CF8M	22225.9	53040.6	35.7	67.9
		3/6A	A351 CF8M	23008.0	53182.8	39.7	63.2
90 DEG HALF ELBOW	4663	3/1	A351 CF8M	23178.6	57733.2	33.3	73.[illegible]
		3/1A	A351 CF8M	23463.0	57448.8	34.6	61.3
90 DEG HALF ELBOW	4747	3/2	A351 CF8M	23747.4	57448.8	34.2	58.3
		3/3	A351 CF8M	23178.6	57022.2	28.9	47.5
90 DEG HALF ELBOW	4898	3/4	A351 CF8M	24174.0	59439.6	39.3	57.3
		3/5	A351 CF8M	24245.1	59724.0	34.4	59.3
90 DEG HALF ELBOW	5089	4/1	A351 CF8M	20988.7	55372.7	39.5	64.2
		4/2	A351 CF8M	21017.2	56254.3	35.8	58.3
90 DEG HALF ELBOW	5839	4/5	A351 CF8M	21244.7	53026.4	31.1	62.3
		4/6	A351 CF8M	21031.4	54107.1	40.0	59.3
90 DEG HALF ELBOW	5247	4/3	A351 CF8M	21400.1	55045.6	33.2	48.7
		4/4	A351 CF8M	21371.6	54931.9	33.9	65.1
40 DEG ELBOW	4541	2/1	A351 CF8M	23463.0	57022.2	22.2	60.3
		2/1A	A351 CF8M	23889.6	57448.8	26.6	57.3
30 DEG ELBOW	4543	5/2	A351 CF8M	22041.0	57448.8	30.0	65.1
		5/3	A351 CF8M	22609.8	57022.2	31.1	55.2
40 DEG ELBOW	5655	2/2	A351 CF8M	21244.7	52756.2	37.8	62.3
		2/2A	A351 CF8M	21258.9	52528.7	37.3	48.7
40 DEG ELBOW	5854	2/3	A351 CF8M	20960.3	54562.1	39.5	67.9
		2/3A	A351 CF8M	21287.3	54107.1	38.6	67.9
50 DEG ELBOW	4594	1/2	A351 CF8M	22894.2	57591.0	34.9	56.2
		1/3A	A351 CF8M	22680.9	57164.4	38.4	64.2
50 DEG ELBOW	4665	1/3	A351 CF8M	22894.2	56453.4	40.9	64.2
		1/3A	A351 CF8M	22680.9	56880.0	43.9	69.6
50 DEG ELBOW	4205	1/1	A351 CF8M	24245.1	57448.8	24.4	56.3
		1/1A	A351 CF8M	24031.8	57591.0	30.3	55.2
30 DEG ELBOW	64422	5/1	A351 CF8M	25169.4	57875.4	25.0	38.0
		5/1A	A351 CF8M	25027.2	58728.6	24.4	60.3

TABLE 4-3

MECHANICAL PROPERTIES OF SA351 CF8M MATERIAL
AT ROOM TEMPERATURE (FROM A TYPICAL PWR PLANT)

PRODUCT FORM	HEAT NR	TEST PIECE NR	MATERIAL	0.2% OFFSET YIELD STRESS (PSI)	ULTIMATE STRENGTH (PSI)	% ELONGATION	% REDUCTION IN AREA
90 DEG HALF ELBOW	4969	3/6	A351 CF8M	33843.6	71811.0	53.3	70.5
		3/6A	A351 CF8M	34270.2	70673.4	43.9	67.8
90 DEG HALF ELBOW	4663	3/1	A351 CF8M	35123.4	71953.2	41.1	63.2
		3/1A	A351 CF8M	34833.0	73659.6	45.1	68.5
90 DEG HALF ELBOW	4747	3/2	A351 CF8M	33701.4	71811.0	47.8	69.5
		3/3	A351 CF8M	34839.0	71100.0	37.8	63.2
90 DEG HALF ELBOW	4898	3/4	A351 CF8M	35123.4	75792.6	36.0	52.2
		3/5	A351 CF8M	36118.8	77072.4	51.8	67.0
90 DEG HALF ELBOW	5089	4/1	A351 CF8M	32137.2	71384.4	44.5	50.2
		4/2	A351 CF8M	31284.0	70673.4	48.1	N/A
90 DEG HALF ELBOW	5839	4/5	A351 CF8M	33132.6	71100.0	47.9	66.5
		4/6	A351 CF8M	32279.4	71526.6	40.5	68.4
90 DEG HALF ELBOW	5247	4/3	A351 CF8M	32420.0	70385.7	41.5	72.0
		4/4	A351 CF8M	32846.6	71096.6	48.6	71.2
40 DEG ELBOW	4541	2/1	A351 CF8M	34981.2	72095.4	37.7	65.0
		2/1A	A351 CF8M	34981.2	71242.2	41.9	66.0
30 DEG ELBOW	4543	5/2	A351 CF8M	33132.6	72522.0	50.7	71.2
		5/3	A351 CF8M	33417.0	72237.6	50.3	67.8
40 DEG ELBOW	5655	2/2	A351 CF8M	35123.4	72237.6	50.7	70.5
		2/2A	A351 CF8M	34128.0	71100.0	47.3	76.2
40 DEG ELBOW	5854	2/3	A351 CF8M	30999.6	72237.6	53.9	71.2
		2/3A	A351 CF8M	31852.8	71100.0	50.4	76.2
50 DEG ELBOW	4594	1/2	A351 CF8M	34128.0	72522.0	49.6	71.2
		1/2A	A351 CF8M	33843.6	72948.6	46.0	77.7
50 DEG ELBOW	4665	1/3	A351 CF8M	33701.4	70246.8	50.6	67.8
		1/3A	A351 CF8M	32279.4	70389.0	51.6	71.2
50 DEG ELBOW	4205	1/1	A351 CF8M	31568.4	76788.0	37.5	61.2
		1/1A	A351 CF8M	38962.8	75508.2	47.0	66.0
30 DEG ELBOW	64422	5/1	A351 CF8M	40669.2	81907.2	43.3	64.0
		5/1A	A351 CF8M	36403.2	71242.2	42.5	71.2

TABLE 4-4

TROJAN MATERIAL PROPERTIES AT 650°F

Material	Pipe SA351 CF8A		Fittings SA351 CF8M	
	σ_y (ksi)	σ_u (ksi)	σ_y (ksi)	σ_u (ksi)
ASME Code minimum	21.0	65.2	18.5	67.0
[				] a,c,e

TABLE 4-5

PRESSURE AND TEMPERATURE CONDITIONS

IN THE PRIMARY LOOP FOR TROJAN

Hot Leg	Temperature:	617°F
	Pressure:	2235 psig
Crossover Leg	Temperature:	552°F
	Pressure:	2200 psig
Cold Leg	Temperature:	553°F
	Pressure:	2290 psig

TABLE 4-6

FRACTURE TOUGHNESS CRITERIA USED IN THE LEAK-BEFORE-BREAK EVALUATION

Location[a]	J_{Ic} (in-lb/in^2)	T_{mat}	J_{max} (in-lb/in^2)
All locations except noted below	[		] a,c,e
3			
7[b]			
9			
11			

a. The locations are shown in figure 3-2.

b. The lower of the values for all the loops are given here.

a,c,e

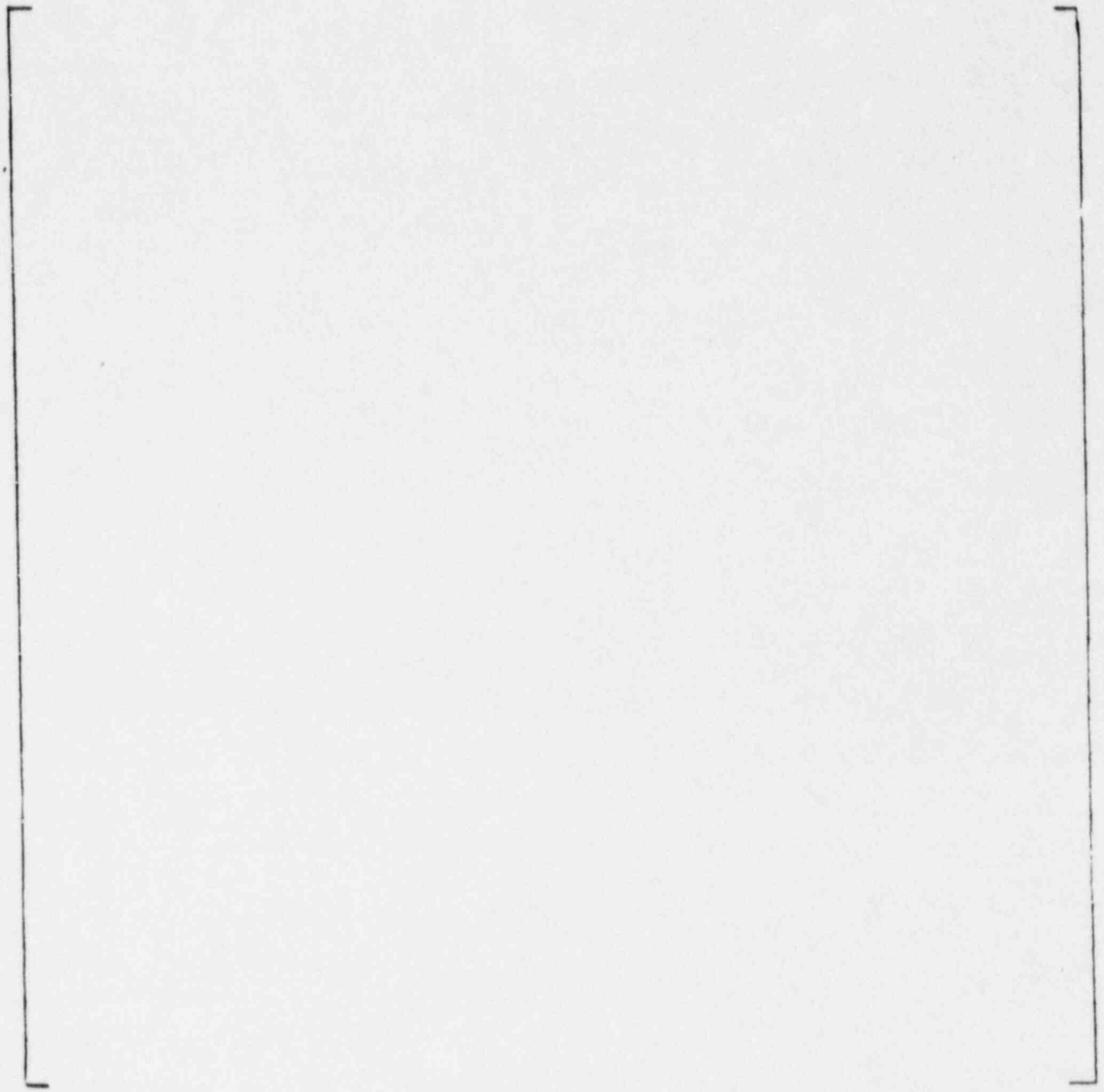

Figure 4-1. True Stress Strain Curve for SA351 CF8A Stainless Steel at 617°F

a,c,e

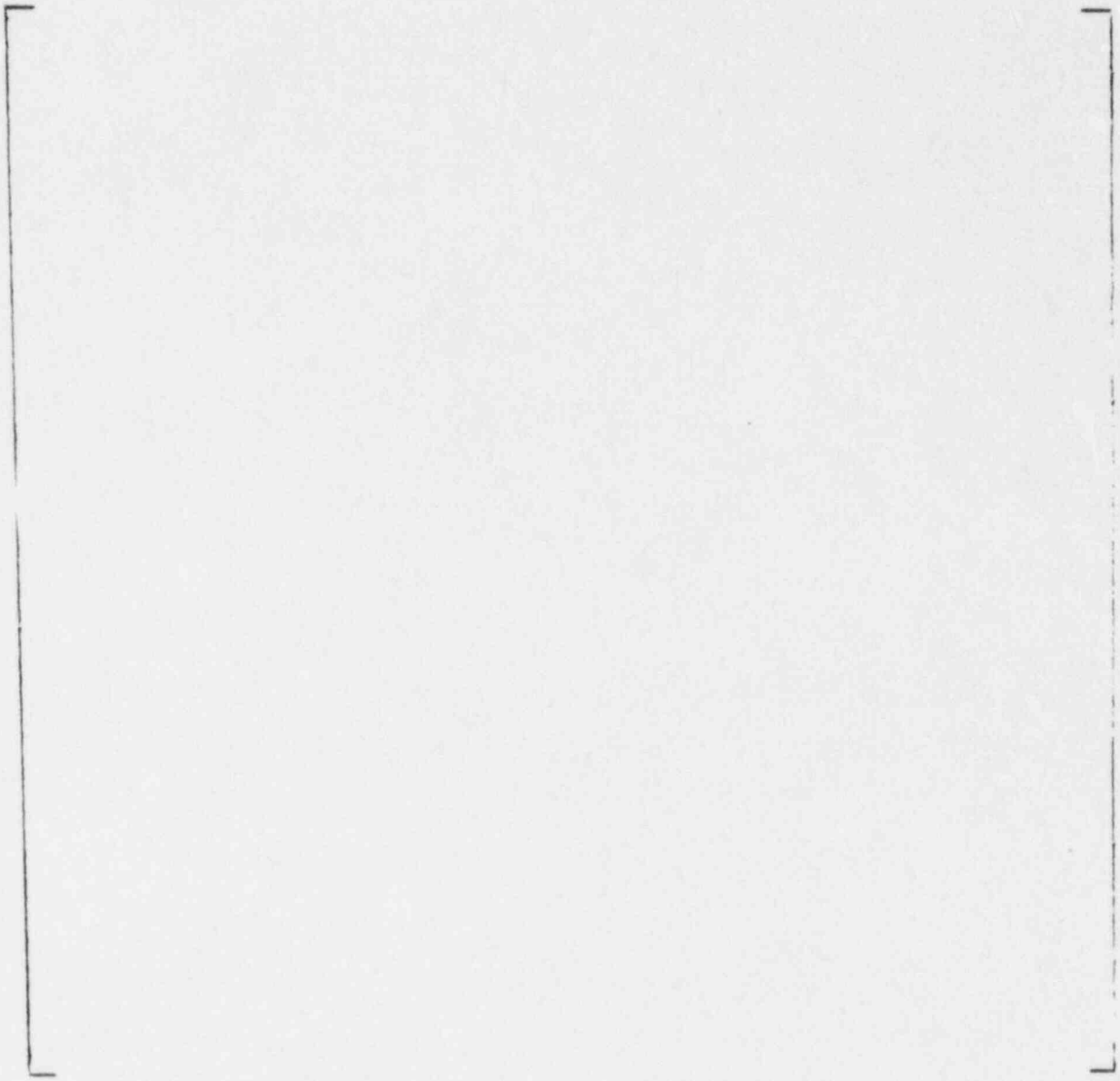

Figure 4-2. True Stress Strain Curve for SA351 CF8A Stainless Steel at 553°F

a,c,e

Figure 4-3. True Stress Strain Curve for SA351 CF8M Stainless Steel at 617°F

a,c,e

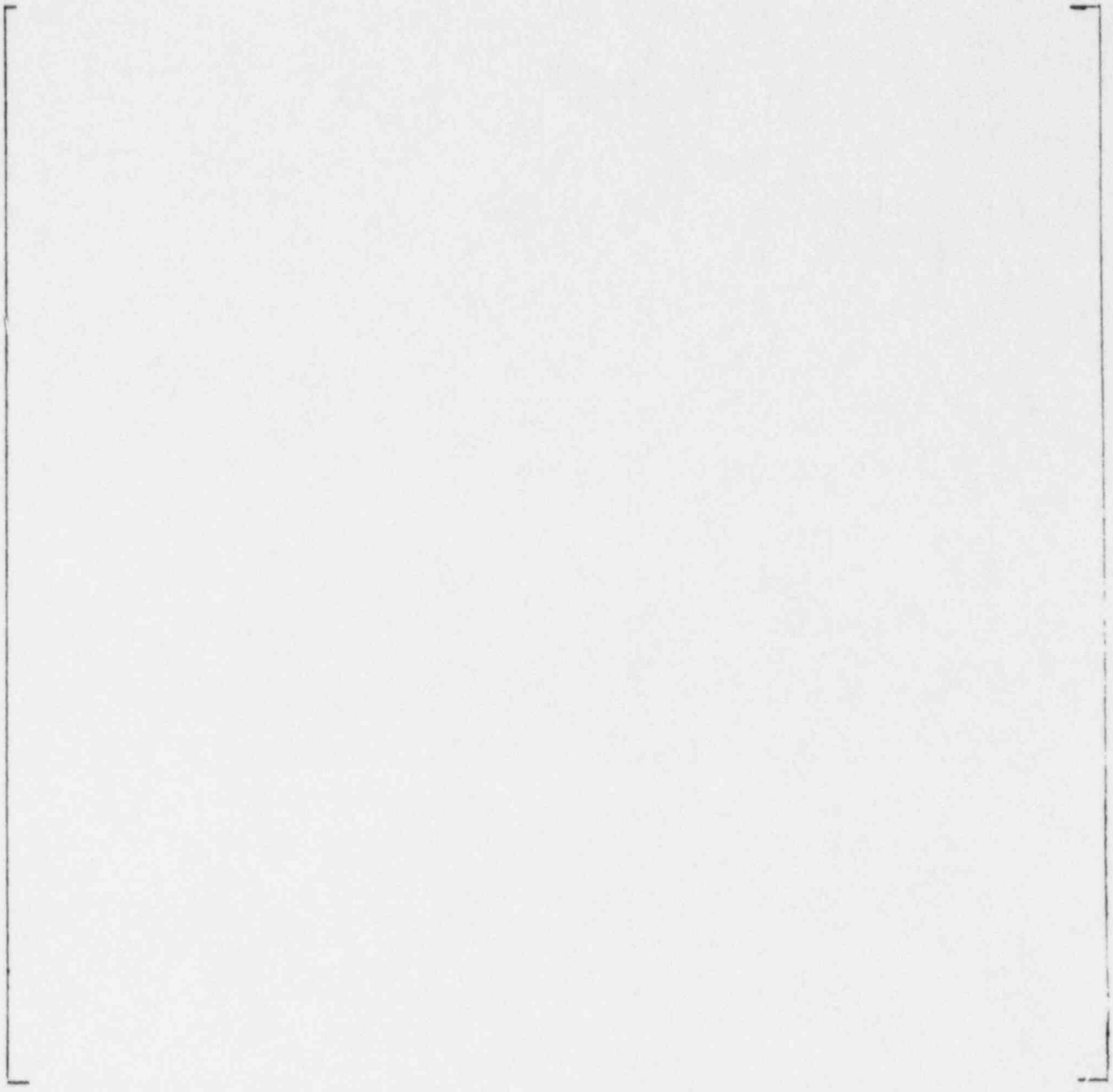

Figure 4-4. True Stress Strain Curve for SA351 CF8M Stainless Steel at 552°F

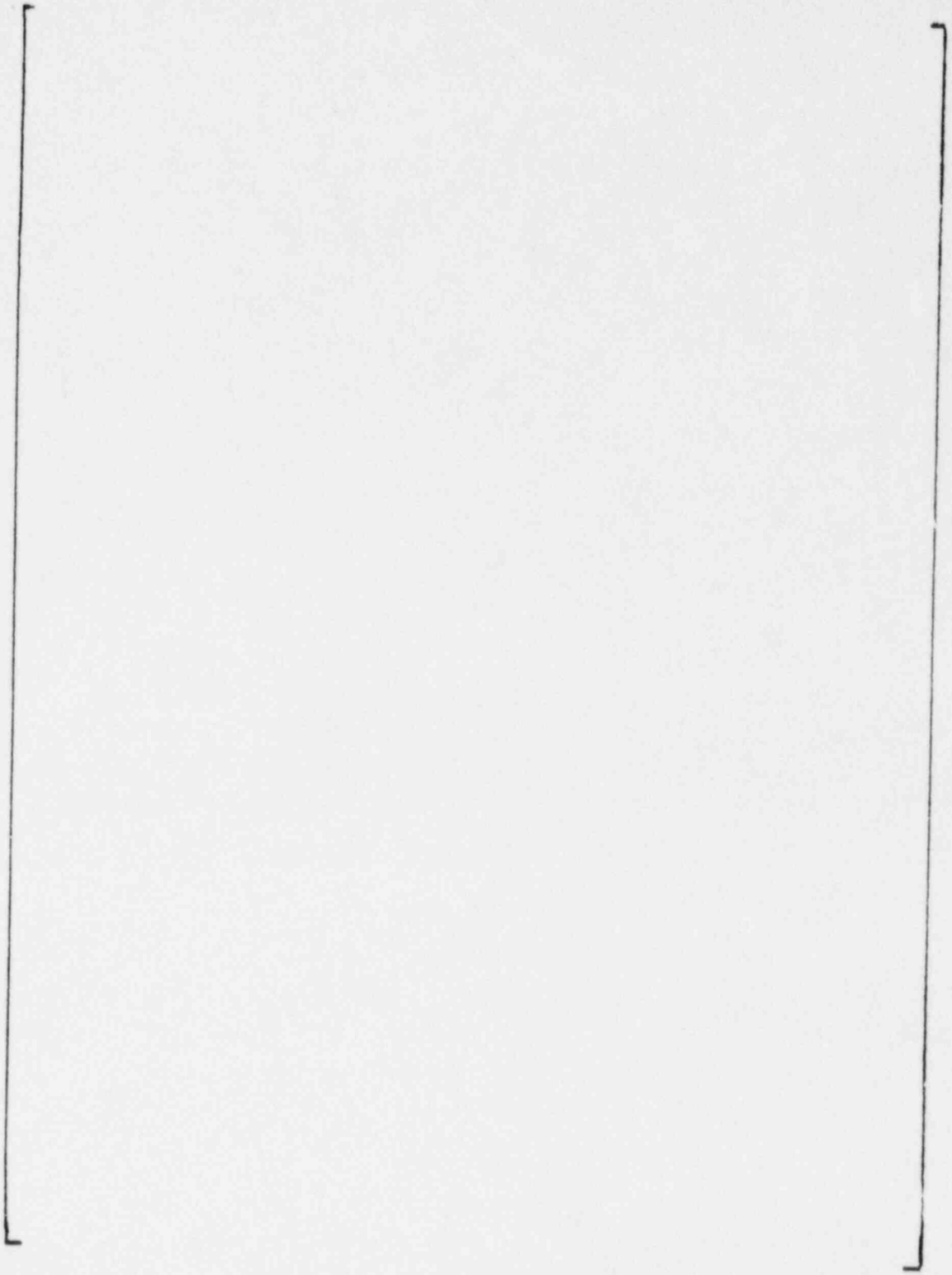

a,c,e

Figure 4-5. J vs Δa for SA351 CF8M Cast Stainless Steel at 600°F

Figure 4-6. J vs. Δa at Different Temperatures for Aged Material [ ]^{a,c,e} (7500 hours at 400°C)

SECTION 5.0
LEAK RATE PREDICTIONS

5.1 Introduction

The purpose of this section is to discuss the method which is used to predict the flow through postulated through-wall cracks and present the leak rate calculation results for through-wall circumferential cracks.

5.2 General Considerations

The flow of hot pressurized water through an opening to a lower back pressure causes flashing which can result in choking. For long channels where the ratio of the channel length, L, to hydraulic diameter, D_H, (L/D_H) is greater than [ ]^{a,c,e}, both [

]^{a,c,e}.

5.3 Calculation Method

The basic method used in the leak rate calculations is the method developed by [

]^{a,c,e}.

The flow rate through a crack was calculated in the following manner. Figure 5-1 from reference 5-1 was used to estimate the critical pressure, Pc, for the primary loop enthalpy condition and an assumed flow. Once Pc was found for a

given mass flow, the [ ]^{a,c,e} was found from figure 5-2 taken from reference 5-1. For all cases considered, since [ ]^{a,c,e} Therefore, this method will yield the two-phase pressure drop due to momentum effects as illustrated in figure 5-3. Now using the assumed flow rate, G, the frictional pressure drop can be calculated using

$$\Delta P_f = [\quad]^{a,c,e} \qquad (5\text{-}1)$$

where the friction factor f is determined using the [ ]^{a,c,e} The crack relative roughness, ε, was obtained from fatigue crack data on stainless steel samples. The relative roughness value used in these calculations was [ ]^{a,c,e}

The frictional pressure drop using Equation 5-1 is then calculated for the assumed flow and added to the [ ]^{a,c,e} to obtain the total pressure drop from the primary system to the atmosphere. That is, for the primary loop

$$\text{Absolute Pressure} - 14.7 = [\quad]^{a,c,e} \qquad (5\text{-}2)$$

for a given assumed flow G. If the right-hand side of Equation 5-2 does not agree with the pressure difference between the primary loop and the atmosphere, then the procedure is repeated until Equation 5-2 is satisfied to within an acceptable tolerance and this results in the flow value through the crack. This calculational procedure has been recommended by [ ]^{a,c,e} for this type of [ ]^{a,c,e} calculation.

5.4 Leak Rate Calculations

Leak rate calculations were made as a function of crack length for all the five critical locations previously identified. The normal operating loads of table 3-1 were applied in these calculations. The crack opening area was estimated using the method of reference 5-3 and the leak rate was calculated using the two-phase flow formulation described above.

The flaw sizes to yield a leak rate of 10 gpm at each of the locations were established and are summarized in table 5-1.

5.5 References

5-1 [

]a,c,e.

5-2 [

]a,c,e.

5-3 Tada, H., "The Effects of Shell Corrections on Stress Intensity Factors and the Crack Opening Area of Circumferential and a Longitudinal Through-Crack in a Pipe," Section II-1, NUREG/CR-3464, September 1983.

TABLE 5-1

LEAK RATE RESULTS

Location	10 gpm Flaw Size (in.)
1	[ ] a,c,e
3	
7	
9	
11	

Figure 5-1 Analytical Predictions of Critical Flow Rates of Steam-Water Mixtures

[a,c,e

CRITICAL PRESSURE RATIO (p_c/p_o)

]a,c,e

Figure 5-2 [ ]a,c,e Pressure Ratio as a Function of L/D

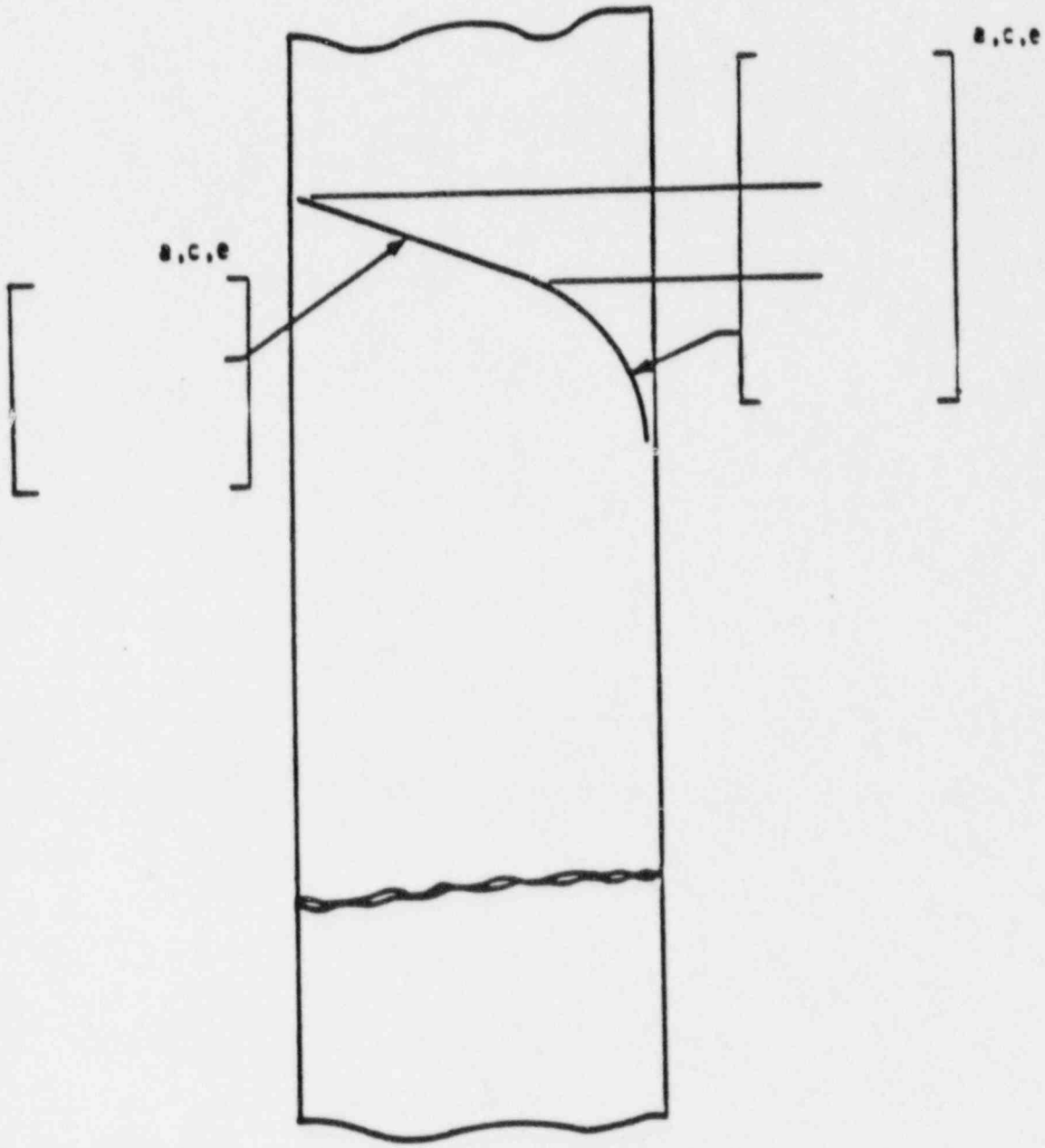

Figure 5-3. Idealized Pressure Drop Profile Through a Postulated Crack

SECTION 6.0
FRACTURE MECHANICS EVALUATION

6.1 Local Failure Mechanism

The local mechanism of failure is primarily dominated by the crack tip behavior in terms of crack-tip blunting, initiation, extension and finally crack instability. Depending on the material properties and geometry of the pipe, flaw size, shape and loading, the local failure mechanisms may or may not govern the ultimate failure.

The local stability will be assumed if the crack does not initiate at all. It has been accepted that the initiation toughness measured in terms of J_{Ic} from a J-integral resistance curve is a material parameter defining the crack initiation. If, for a given load, the calculated J-integral value is shown to be less than the J_{Ic} of the material, then the crack will not initiate. If the initiation criterion is not met, one can calculate the tearing modulus as defined by the following relation:

$$T_{app} = \frac{dJ}{da} \quad \frac{E}{\sigma_f^2}$$

where:

T_{app} = applied tearing modulus
E = modulus of elasticity
σ_f = [ ]^{a,c,e} (flow stress)
a = crack length

[ ]^{a,c,e}

Stability is said to exist when ductile tearing occurs i.e., T_{app} is less than T_{mat}, the experimentally determined tearing modulus.

In summary, the local crack stability will be established by the two-step criteria:

$$J < J_{Ic}$$

or

$$T_{app} < T_{mat} \quad \text{if } J \geq J_{Ic}$$

and $J \leq J_{max}$

6.2 Global Failure Mechanism

Determination of the conditions which lead to failure in stainless steel should be done with plastic fracture methodology because of the large amount of deformation accompanying fracture. One method for predicting the failure of ductile material is the plastic instability method, based on traditional plastic limit load concepts, but accounting for strain hardening and taking into account the presence of a flaw. The flawed pipe is predicted to fail when the remaining net section reaches a stress level at which a plastic hinge is formed. The stress level at which this occurs is termed as the flow stress. The flow stress is generally taken as the average of the yield and ultimate tensile strength of the material at the temperature of interest. This methodology has been shown to be applicable to ductile piping through a large number of experiments and will be used here to predict the critical flaw size in the primary coolant piping. The failure criterion has been obtained by requiring equilibrium of the section containing the flaw (figure 6-1) when loads are applied. The detailed development is provided in appendix A for a through-wall circumferential flaw in a pipe with internal pressure, axial force, and imposed bending moments. The limit moment for such a pipe is given by:

[ ] a,c,e

where:

[

]a,c,e

[

]a,c,e

The analytical model described above accurately accounts for the piping internal pressure as well as imposed axial force as they affect the limit moment. Good agreement was found between the analytical predictions and the experimental results (reference 6-1).

6.3 Results of Crack Stability Evaluation

Stability analyses were performed at the load critical and toughness critical locations defined in section 3. The elastic-plastic fracture mechanics (EPFM) J-integral analyses for through-wall circumferential cracks in a cylinder were performed using the procedure in the EPRI fracture mechanics handbook (reference 6-2). The lower-bound material properties of section 4.0 were used.

The results of the EPFM analyses are given in tables 6-1 and 6-2. The critical toughness criteria established in section 4.3 were used. The normal plus SSE loads given in table 3-2 were used for these calculations.

Two margin conditions were evaluated. First the leakage flaw (i.e. the flaw yielding a leakage of 10 gpm) was doubled and EPFM analyses were performed for normal plus SSE loadings. The applied tearing modulus was calculated from the EPFM results (elastic-plastic load controlled J-T analysis) using

$$T_{app} = \frac{dJ}{da}\frac{E}{\sigma_f^2}$$

where E is the modulus of elasticity and σ_f is the flow stress taken as the average of the yield and ultimate strength. In table 6-1 the calculated values are seen to be well below the critical toughness values. J_{Ic} is exceeded only at locations 1 and 11.

Similar analyses were made using the leakage flaws with the normal plus SSE loads (from table 3-2) increased by a factor of 1.4. These results are provided in table 6-2. As noted in the table a margin of 1.4 on normal plus SSE loads for leakage flaws is demonstrated at all locations except location . where only a margin of 1.2 is demonstrated. To additionally evaluate location 1, the loads were combined using the absolute load combination method (ee section 3.3) as outlined in SRP 3.6.3. The absolute load combination resulted in F_x = 2235 kips and M_b = 34,716 in-kips. Based on these loads, the $J_{applied}$ was calculated to be [ ]^{a,c,e} and $T_{applied}$ was calculated to be [ ]^{a,c,e}. Thus the results of table 6-2 demonstrate margins on applied loads.

SRP 3.6.3 requires the same load combination procedure be used when addressing margin on flaw size and margin on load. Thus the loads obtained by the absolute load combination method were used to evaluate margin on flaw size. The results are also given in table 6-1 where it is seen that a margin of 1.5 on the leakage size flaw is obtained. For a factor of two on flaw size, the load based on the absolute load combination method is met at the 94 percent level as indicated.

From table 6-1 it is clear that the limiting location is location 1 (the critical flaw size is the smallest at this location). Global stability analysis was performed at this location as described in section 6.2. Figure 6-2 shows a plot of the plastic limit moment as a function of through-wall circumferential flaw length in the hot leg (location 1). The maximum applied bending moment can be plotted on this figure and used to determine a critical flaw length, which is shown to be [ ]^{a,c,e} inches.

In summary it is seen that large margins exist for both flaw and load at all locations except location 1. The margin on flaw size based on normal plus SSE is well demonstrated, however the corresponding margin on load is 1.2, not

1.4. Conversely, using the absolute load combination method, the margin on load is well demonstrated with the margin on flaw size being 1.5, not 2. The adequacy of the margins demonstrated at location 1 is discussed below.

First the reason why the sought after margins at location 1 were not demonstrated is discussed. This is perhaps best simply demonstrated by referring to figure 4-1. Taking the applied stress as the effective stress, the normal plus SSE load (stress of 26.98 ksi) produces an unflawed outside surface strain of about 1.25 percent. Also, 1.4 times 26.98 ksi is 37.78 ksi which yields a strain of about 6%. That is, at the load level in question, half an order-of-magnitude increase in the applied strain results from only a 40 percent increase in load. For a factor of 1.2 on normal plus SSE load the strain is 3.7 percent. For the loads from the absolute load combination method the stress is 30.1 ksi, a 11 percent increase over the normal plus SSE load. The corresponding strain is 2.6%. At 94% of this load the strain is 2.0 percent (see footnotes of table 6-1). Overall the applied fracture toughness results discussed above are not particularly surprising.

Next the nature of the loads themselves is examined. A very large percentage of the bending moment is due to thermal expansion, a displacement controlled load. Likewise the seismic moment is displacement controlled considering damping. Consequently, displacement or strain is a better overall stability criterion for displacement controlled stresses. Of course in the elastic region, load control and displacement control stress criteria are equivalent.

It appears plausible then to examine margins in terms of strain at Location 1. The established margin on load wherein the margin is 1.2 (see table 6-2), gives a margin of almost three (~3.7/1.25) in strain. For the 6.8 inch long flaw of table 6-1 subjected to 94 percent of the load obtained by the absolute load combination method, the strain is 2.0 percent or 60 percent greater than the strain for normal plus SSE load. The stability for the flaw size with a 60 percent increase in strain over that for normal plus SSE load contrasts with the 11% differences in stress for the two loads under discussion.

An alternative to meeting precisely the margins has been discussed above.

For the Trojan plant, it is believed that a sufficient basis has been established for using engineering judgment and flexibility in assessing these results. This is consistent with NUREG-1061, Volume 3, page 5-21.

Supplementing the above discussion concerning location 1 it should be kept in mind that conservative or benchmarked procedures have been applied in every step of the evaluation. The loads are conservatively calculated and combined. The fracture toughness criteria at location 1 are taken equal to that of [ ]^{a,c,e} while in fact the fracture toughnesses would be considerably higher based on KCU values. Thus margins are in fact greater than those established in the above discussion.

6.4 References

6-1. Kanninen, M. F., et. al., "Mechanical Fracture Predictions for Sensitized Stainless Steel Piping with Circumferential Cracks," EPRI NP-192, September 1976.

6-2. Kumar, V., German, M. D. and Shih, C. P., "An Engineering Approach for Elastic-Plastic Fracture Analysis," EPRI Report NP-1931, Project 1237-1, Electric Power Research Institute, July 1981.

TABLE 6-1

RESULTS OF STABILITY ANALYSES - MARGIN ON FLAW SIZE

Location	J_{Ic} (in-lb/in^2)	T_{mat}	J_{max} (in-lb/in^2)	Crack Length (in)	J_{app} (in-lb/in^2)	T_{app}
Normal Plus SSE Loading						
1	[					] a,c,e
3						
7						
9						
11	[					]
Load by Absolute Load Combination Method						
1	[					] a,c,e
1	[					]

a NA - not applicable

b This crack length is 1.5 times that of the leakage flaw.

c For this crack depth, the load used is 94% of the load obtained by the absolute load combination method and 4% greater than normal plus SSE load, noting that the stresses for the two loads in question differ by only 11 percent.

TABLE 6-2

RESULTS OF STABILITY ANALYSES - MARGIN ON LOADS

Location	J_{Ic} (in-lb/in^2)	T_{mat}	J_{max} (in-lb/in^2)	Crack Length (in)	J_{app} (in-lb/in^2)	T_{app}
Factor of 1.4 on Load Obtained by SRSS Combination						
1[a]	[					] a,c,e
3						
7						
9						
11						
Load by Absolute Load Combination Method						
1	[					] a,c,e

[a] These results are for a load of 1.2 times the normal plus SSE load not 1.4 times the normal plus SSE load.

[b] NA - not applicable

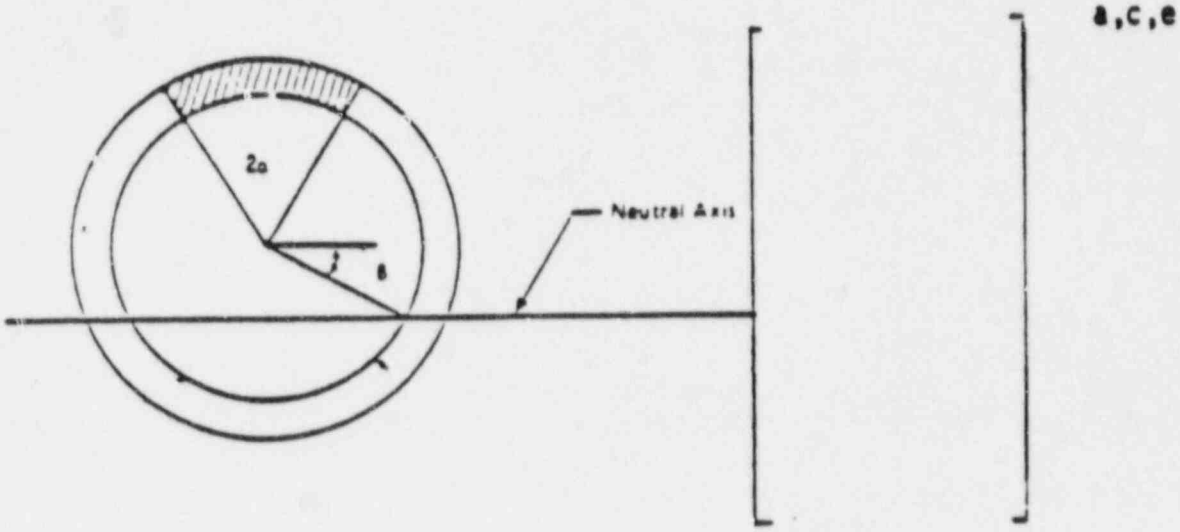

Figure 6-1. [ ]^{a,c,e} Stress Distribution

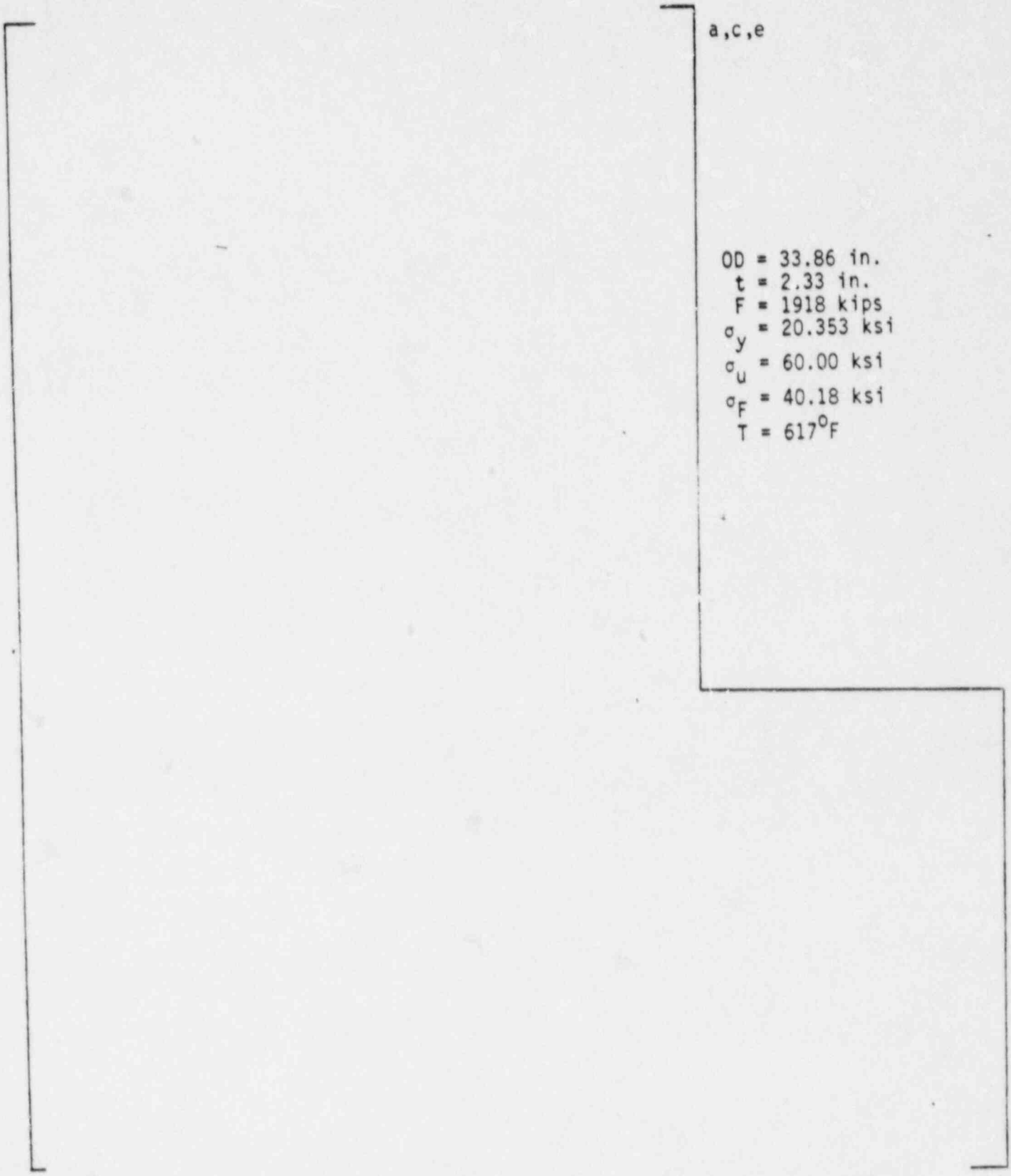

Figure 6-2. "Critical" Flaw Size Prediction - Hot Leg at Critical Location 1

SECTION 7.0
FATIGUE CRACK GROWTH ANALYSIS

To determine the sensitivity of the primary coolant system to the presence of small cracks, a fatigue crack growth analysis was carried out for the [ ]^{a,c,e} region of a typical system (see Location [ ]^{a,c,e} of figure 3-2). This region was selected because crack growth calculated here will be typical of that in the entire primary loop. Crack growths calculated at other locations can be expected to show less than 10% variation.

A [ ]^{a,c,e} of a plant typical in geometry and operational characteristics to any Westinghouse PWR System. [ ]^{a,c,e} All normal, upset, and test conditions were considered. A summary of the applied transients is provided in table 7-1. Circumferentially oriented surface flaws were postulated in the region, assuming the flaw was located in three different locations, as shown in figure 7-1. Specifically, these were:

Cross Section A: [ ]^{a,c,e}
Cross Section B: [ ]^{a,c,e}
Cross Section C: [ ]^{a,c,e}

Fatigue crack growth rate laws were used [ ]^{a,c,e} The law for stainless steel was derived from reference 7-1, with a very conservative correction for the R ratio, which is the ratio of minimum to maximum stress during a transient.

For stainless steel, the fatigue crack growth formula is:

$$\frac{da}{dn} = (5.4 \times 10^{-12}) K_{eff}^{4.48} \text{ inches/cycle}$$

where $K_{eff} = K_{max} (1-R)^{0.5}$

$R = K_{min}/K_{max}$

[

a,c,e

]

where: [ ]a,c,e

The calculated fatigue crack growth for semi-elliptic surface flaws of circumferential orientation and various depths is summarized in table 7-2, and shows that the crack growth is very small, [ ]a,c,e

7.1 References

7-1 Bamford, W. H., "Fatigue Crack Growth of Stainless Steel Piping in a Pressurized Water Reactor Environment," Trans. ASME Journal of Pressure Vessel Technology, Vol. 101, Feb. 1979.

7-2 [

]a,c,e

7-3 [

]a,c,e

TABLE 7-1

SUMMARY OF REACTOR VESSEL TRANSIENTS

NUMBER	TYPICAL TRANSIENT IDENTIFICATION	NUMBER OF CYCLES
	Normal Conditions	
1	Heatup and Cooldown at 100°F/hr (pressurizer cooldown 200°F/hr)	200
2	Load Follow Cycles (Unit loading and unloading at 5% of full power/min)	18300
3	Step load increase and decrease	2000
4	Large step load decrease, with steam dump	200
5	Steady state fluctuations	10^6
	Upset Conditions	
6	Loss of load, without immediate turbine or reactor trip	80
7	Loss of power (blackout with natural circulation in the Reactor Coolant System)	40
8	Loss of Flow (partial loss of flow, one pump only)	80
9	Reactor trip from full power	400
	Test Conditions	
10	Turbine roll test	10
11	Primary Side Hydrostatic test conditions	50
12	Cold Hydrostatic test	10

TABLE 7-2

TYPICAL FATIGUE CRACK GROWTH AT
[ ]^{a,c,e} (40 YEARS)

	FINAL FLAW (in)		
INITIAL FLAW (IN)	[ ]^{a,c,e}	[ ]^{a,c,e}	[ ]^{a,c,e}
0.292	0.31097	0.30107	0.30698
0.300	0.31949	0.30953	0.31626
0.375	0.39940	0.38948	0.40763
0.425	0.45271	0.4435	0.47421

[ ]a,c,e

Figure 7-1. Typical Cross-Section of [ ]a,c,e

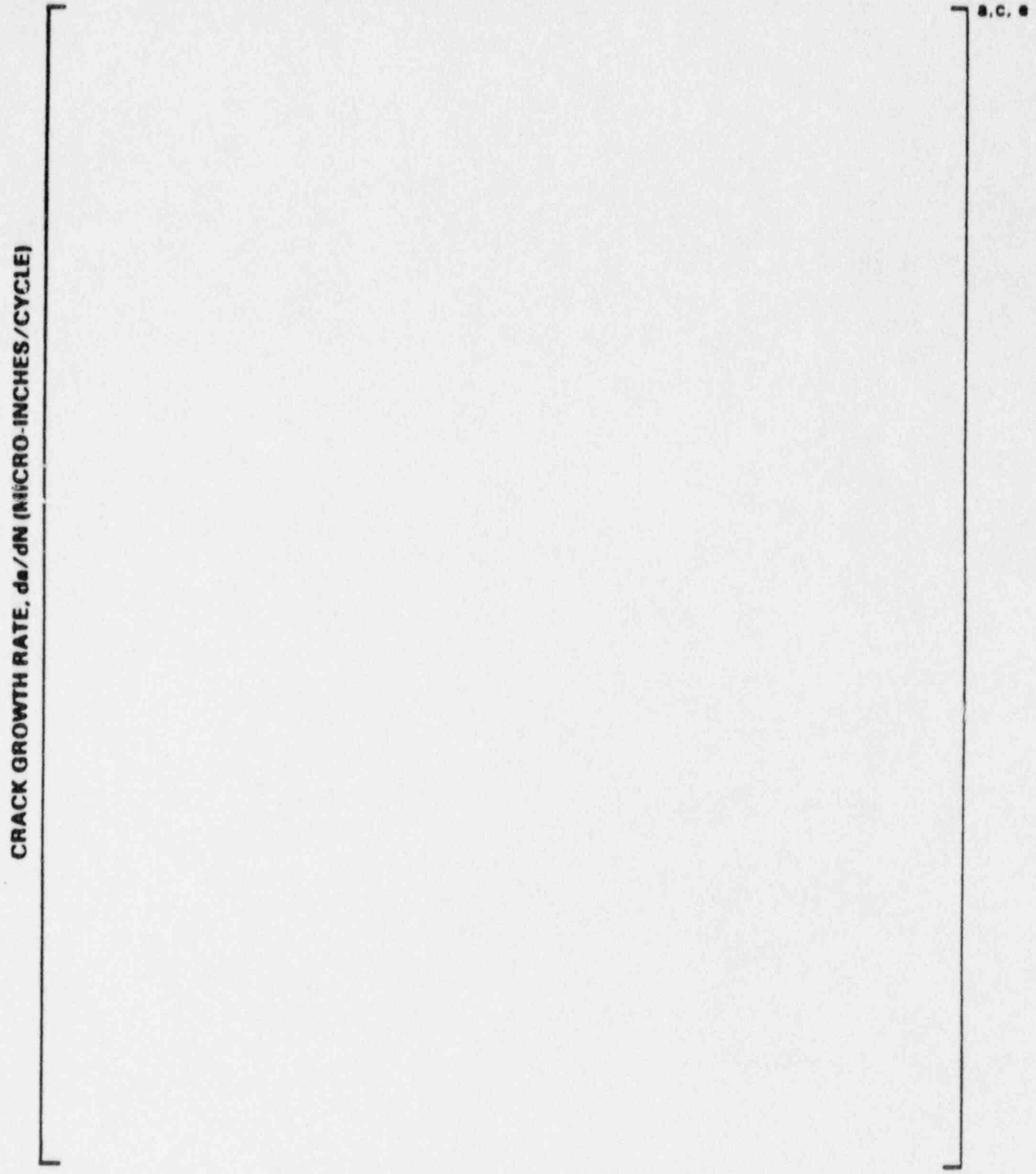

Figure 7-2. Reference Fatigue Crack Growth Curves for [
]a,c,e

[a,c,e]

Figure 7-3. Reference Fatigue Crack Growth Law for [ ]^{a,c,e} in a Water Environment at 600°F

SECTION 8.0
ASSESSMENT OF MARGINS

The results of the leak rates of section 5.4 and the corresponding fracture toughness evaluations of section 6.3 are used in performing the assessment of margins.

At the load critical location (location 1), J_{app} and T_{app} for a [ ]^{a,c,e} long through-wall circumferential flaw are found to be [ ]^{a,c,e} and [ ]^{a,c,e}, respectively. The T_{app} is shown to be less than T_{mat} of [ ]^{a,c,e} and J_{app} is shown to be less than J_{max} of [ ]^{a,c,e} in-lb/in^2. A [ ]^{a,c,e} inch flaw yields a leak rate of 10 gpm. Thus at the load critical location, there is a margin of at least two between the flaw size yielding a leak rate of 10 gpm and the critical flaw size [ ]^{a,c,e}. In addition, the leakage size flaw of [ ]^{a,c,e} is shown to be stable when subjected to maximum loads obtained by the absolute sum load combination method as suggested by SRP 3.6.3. Stability for the leakage size flaw was not established using a factor of 1.4 on the normal plus SSE load. A factor of 1.2 was established however. Stability of a flaw twice the size of the leakage size flaw was demonstrated at 94 percent of the load obtained by the absolute sum load combination method. Stability was also established for this load for a flaw 1.5 times the leakage flaw size.

Because most of the normal plus SSE bending moment is displacement controlled an evaluation based on strain was made. Using strain as a criterion, a factor of three on strain exists for the factor of 1.2 on load. Similarly a factor of 1.60 on strain exists for a flaw twice the leakage size flaw which was stable at 94 percent of the load obtained by the absolute load combination method. Overall it is judged that adequate margins on flaw size and load have been demonstrated at location 1 consistent with the philosophy of NUREG 1061, Vol. 3.

At the remaining four toughness critical locations a flaw up to at least [ ]^{a,c,e} inches long is stable. A margin of at least 2 is demonstrated between the flaw size yielding a leakage of 10 gpm and the critical flaw size. The normal plus SSE loads are increased by a factor of $\sqrt{2}$

and crack stability is demonstrated for the leakage size flaws (i.e. flaws yielding a leakage of 10 gpm). Thus the margin on loads is demonstrated.

In section 6.3 the "maximum" flaw size at the load critical location (limiting location) using the limit load method is found to be at least [ ]^{a,c,e} inches. Thus, based on the above paragraphs, the critical flaw sizes at these locations would exceed [ ]^{a,c,e} respectively.

In summary, relative to

1. Flaw Size

   a. A margin of at least 2 exists between the critical flaw and the flaw yielding a leak rate of 10 gpm.

   b. If limit load is used as the basis for critical flaw size, the margin for global stability well exceeds that based on local stability fracture mechanics evaluation.

2. Leak Rate

   A margin of 10 exists between the calculated leak rate from the "leakage-size flaws" and a leak detection capability of 1 gpm. The capability of each of the pressure boundary leak detection systems are given in table 5.2-9 of the Trojan FSAR.

3. Loads

   a. The J_{app} values for the Trojan plant are enveloped by the toughness allowables established for thermally aged material.

   b. At load critical location the leakage size flaw was shown to be stable when subjected to normal plus SSE loads obtained by absolute summation of individual components. This method of combination results in maximum load at the location of interest.

c. At toughness critical locations the leakage-size flaws were shown to be stable when subjected to 2 times the normal plus SSE loads.

4. General (Load Critical Location)

a) Margin criteria on both flaw size and load were not met at the load critical location using a specific procedure for calculating normal plus SSE loads.

b) For the normal plus SSE load obtained by the absolute sum combination method, a factor of 1.5 on the leakage size flaw was established as compared to a target of 2. For a factor of 2 on flaw size, stability was established at 94 percent of the load.

c) A factor of 1.2 on load was established as compared to a target of 1.4.

d) Using strain as a criterion, a factor of 1.6 was established for the 94 percent load of item 4b). For the 1.2 factor of item 4c), a factor of 3 on strain was established.

e) The margins established at the load critical locations are judged adequate consistent with the philosophy of NUREG 1061, Volume 3.

SECTION 9.0
CONCLUSIONS

This report justifies the elimination of RCS primary loop pipe breaks for the Trojan plant as follows:

a. Stress corrosion cracking is precluded by use of fracture resistant materials in the piping system and controls on reactor coolant chemistry, temperature, pressure, and flow during normal operation.

b. Water hammer should not occur in the RCS piping because of system design, testing, and operational considerations.

c. The effects of low and high cycle fatigue on the integrity of the primary piping are negligible.

d. Adequate margin exists between the leak rate of small stable flaws and the capability of the Trojan plant's reactor coolant system pressure boundary Leakage Detection System.

e. Ample margin exists between the small stable flaw sizes of item d and larger stable flaws.

f. Ample margin exists in the material properties used to demonstrate end-of-service life (relative to aging) stability of the critical flaws.

For each critical location a flaw is identified that will be stable because of the ample margins in d, e, and f above.

Based on the above, it is concluded that dynamic effects of RCS primary loop pipe breaks need not be considered in the structural design basis of the Trojan plant.

APPENDIX A

LIMIT MOMENT

[

] a,c,e

FIGURE A-1 PIPE WITH A THROUGH-WALL CRACK IN BENDING

APPENDIX B

ALTERNATE TOUGHNESS CRITERIA FOR THE TROJAN CAST PRIMARY LOOP COMPONENTS

B.1 INTRODUCTION

Not all of the individual cast piping components of the Trojan primary loop piping satisfy the original [ ]^{a,c,e} criteria (reference 4-3). In this appendix, the alternate toughness criteria for thermally aged cast stainless steel developed in reference 4-5 will be used to categorize the various individual cast piping components thus establishing criteria based upon which the mechanistic pipe break evaluation may be performed. Reference 4-5 has been reviewed by the NRC wherein the NRC concluded that reference 4-5 may be utilized for establishing the fracture criteria for thermally aged cast stainless piping applicable for the leak-before-break analyses (reference B-1). First the chemistry and calculated room temperature Charpy U-notch energy (KCU), values are given followed by an identification of each of the heats of material which did not meet the [ ]^{a,c,e} criteria and their location.

B.2 CHEMISTRY AND KCU TOUGHNESS

The correlation of reference 4-4 which is based on the chemistry of the cast stainless steel piping was used to calculate the associated KCU value. The chemistry and end-of-service life KCU toughness values are given in table B-1. Of the forty-seven heats of cast stainless steel, five fail to meet the current [ ]^{a,c,e} criteria. These heats occur in the fittings of the hot, and crossover legs and in the cold leg pipe.

B.3 THE AS-BUILT TROJAN LOOPS

Trojan is a four-loop Westinghouse type pressurized water reactor plant. A typical four-loop primary system is sketched in figure B-1. The loops are identified as Loops 1, 2, 3 and 4 in the Trojan plant. Sketches for associating piping components which have toughnesses less than that of [ ]^{a,c,e} are identified (see figures B-2 to B-4).

B.4 ALTERNATE TOUGHNESS CRITERIA FOR THE TROJAN PRIMARY LOOP MATERIAL ON A COMPONENT BY COMPONENT BASIS

The alternate toughness criteria for the Trojan cast primary loop material may be obtained by applying the methodology of reference 4-5 to table B-1. First, it is observed that 42 of the 47 heats fall into category 1, i.e., they are at least as tough as [ ]^{a,c,e}. The remaining five heats fall into category 2. Typical toughness calculations using the methodology of reference 4-5 are given below for a category 2 heat.

The 90 degree elbow on crossover leg [ ]^{a,c,e} has the lowest calculated end-of-service life KCU at room temperature of [ ]^{a,c,e} daJ/cm^2 which falls below that of [ ]^{a,c,e}. The δ-ferrite content is [ ]^{a,c,e}. By reference 4-5, the [

]^{a,c,e} Since the end-of-service life KCU exceeds the fully aged KCU, the heat falls into category 2. Thus:

J_{Ic} = [ ]^{a,c,e}

T_{mat} = [ ]^{a,c,e}

and

J_{max} = [ ]^{a,c,e}

These toughness results and the results for the remaining heats which do not meet the [ ]^{a,c,e} criteria are summarized in table B-2.

B.5 REFERENCES

B-1 Letter: Dominic C., DiIanni, NRC to D. M. Muslof, Northern States Power Company, dated December 22, 1986, Docket Nos. 50-282 and 50-306.

TABLE B-1

CHEMISTRY AND CALCULATED KCU VALUES FOR EACH PRIMARY LOOP PIPING
OF THE TROJAN NUCLEAR PLANT

[ ] a,c,e

TABLE B-1 (cont.)

CHEMISTRY AND CALCULATED KCU VALUES FOR EACH PRIMARY LOOP PIPING
OF THE TROJAN NUCLEAR PLANT

a,c,e

TABLE B-1 (cont.)

CHEMISTRY AND CALCULATED KCU VALUES FOR EACH PRIMARY LOOP PIPING
OF THE TROJAN NUCLEAR PLANT

[a,c,e]

TABLE B-1 (cont.)

CHEMISTRY AND CALCULATED KCU VALUES FOR EACH PRIMARY LOOP PIPING
OF THE TROJAN NUCLEAR PLANT

[a,c,e]

TABLE B-2

FRACTURE TOUGHNESS CRITERIA FOR THE CAST PRIMARY PIPING
COMPONENTS OF THE TROJAN NUCLEAR PLANT

[ ]a,c,e

* All heats except noted here meet the [ ]a,c,e criteria and therefore will have toughness at least equal to [

]a,c,e

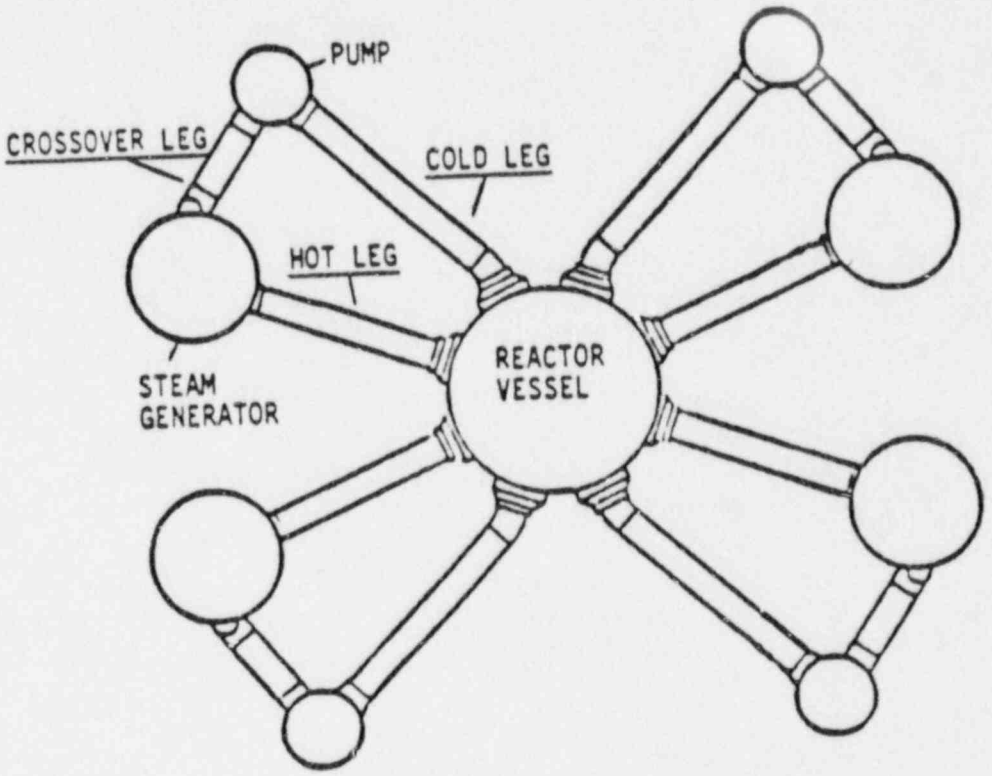

Figure B-1 Typical Layout of the Primary Loops for a Westinghouse Four-Loop Plant Without Isolation Valves

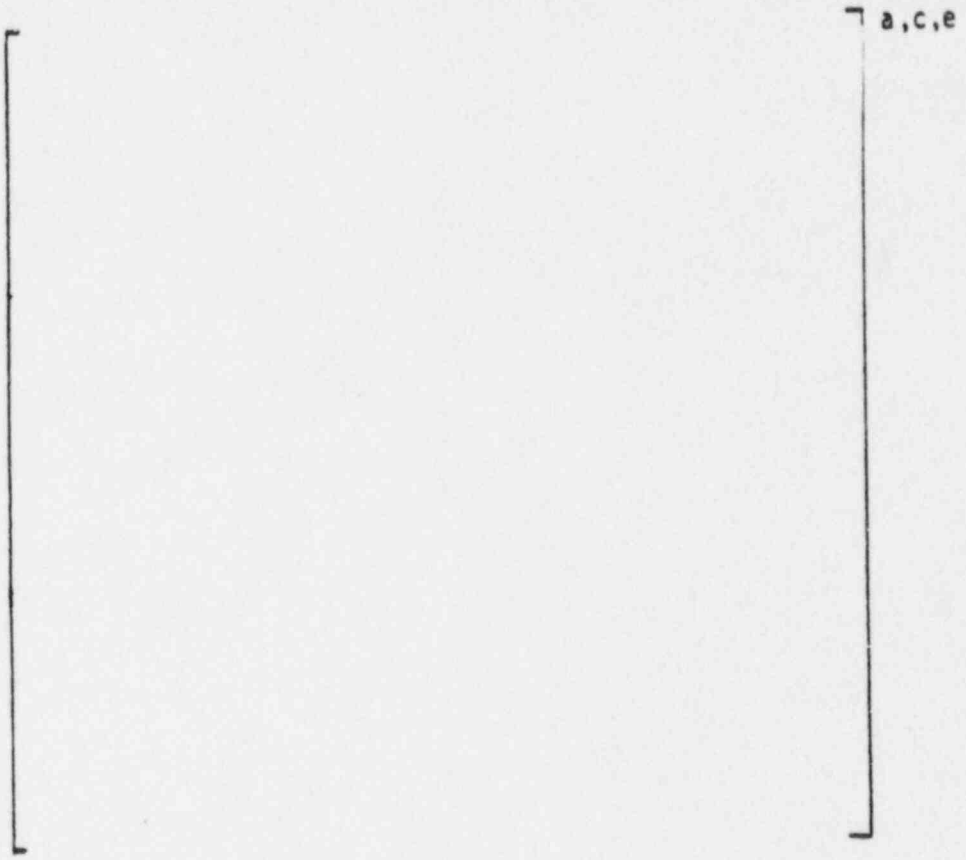

Figure B-2 Identification of Heats with Location for Cold Leg

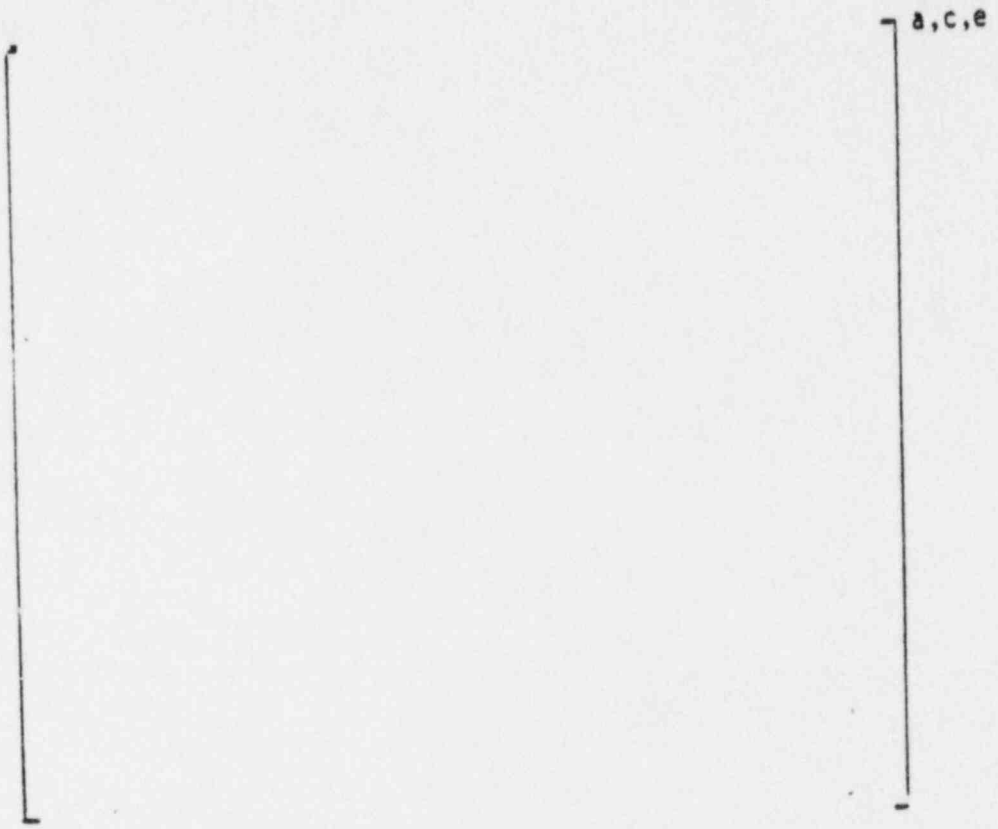

Figure B-3 Identification of Heats with Location for Hot Leg

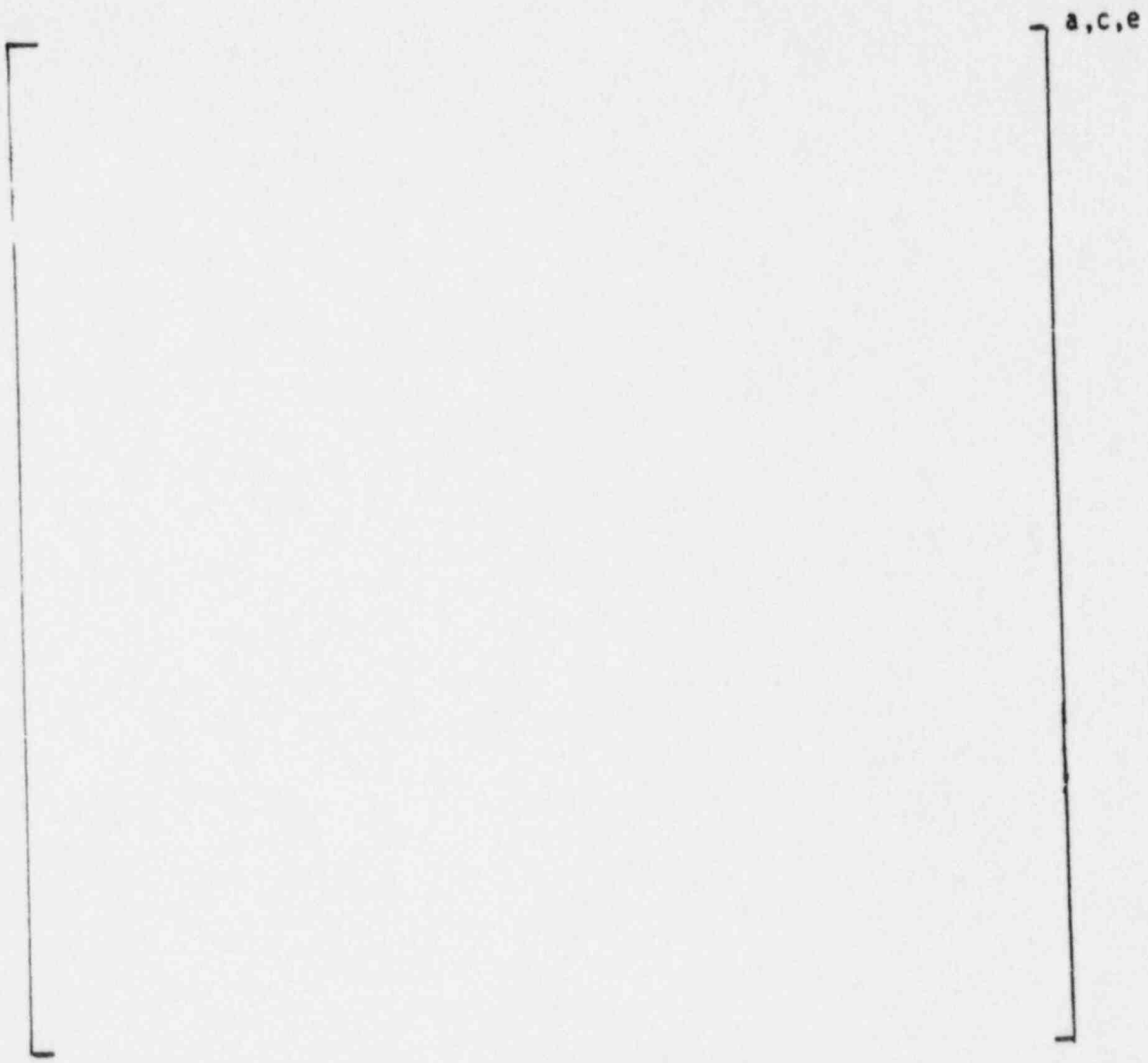

Figure B-4 Identification of Heats with Location for Crossover Leg